



12-1969

Simultaneous Knudsen- and Torsion- Effusion Measurements of the Vapor Pressures of Tetraphenyltin and Hexaphenylditin

Dale Keiser

Follow this and additional works at: https://scholarworks.wmich.edu/masters_theses

 Part of the Chemistry Commons

Recommended Citation

Keiser, Dale, "Simultaneous Knudsen- and Torsion- Effusion Measurements of the Vapor Pressures of Tetraphenyltin and Hexaphenylditin" (1969). *Master's Theses*. 3040.

https://scholarworks.wmich.edu/masters_theses/3040

This Masters Thesis-Open Access is brought to you for free and open access by the Graduate College at ScholarWorks at WMU. It has been accepted for inclusion in Master's Theses by an authorized administrator of ScholarWorks at WMU. For more information, please contact wmu-scholarworks@wmich.edu.



SIMULTANEOUS KNUDSEN- AND TORSION- EFFUSION
MEASUREMENTS OF THE VAPOR PRESSURES OF
TETRAPHENYLTIN AND HEXAPHENYLDITIN

by

Dale Keiser

A Thesis
Submitted to the
Faculty of the School of Graduate
Studies in partial fulfillment
of the
Degree of Master of Arts

Western Michigan University
Kalamazoo, Michigan
December 1969

ACKNOWLEDGEMENTS

During the course of this study I have appreciated the friendship and instruction of Dr. Adli S. Kana'an. I have also benefited from the encouragement of the remainder of my thesis committee, Dr. R. H. Anderson and Dr. D. C. Berndt. Other members of the faculty and fellow students in the Chemistry Department were very generous with their constructive criticism, encouragement, and inspiration. I would like to thank Mr. Richard Durbin and the staff of the machine shop for their indispensable help in construction of the apparatus. I would like to thank the Chemistry Department for supporting me with a teaching assistantship during this work. Finally, I would like to thank my wife for her patience during this time.

MASTER'S THESIS

M-2111

KEISER, Dale
SIMULTANEOUS KNUDSEN- AND TORSION- EFFUSION
MEASUREMENTS OF THE VAPOR PRESSURES OF
TETRAPHENYLTIN AND HEXAPHENYLDITIN.

Western Michigan University, M.A., 1969
Chemistry, general

University Microfilms, Inc., Ann Arbor, Michigan

TABLE OF CONTENTS

CHAPTER I	INTRODUCTION	1
CHAPTER II	THEORY	4
	The Knudsen-Effusion Method	4
	The Torsion-Effusion Method	6
	Correlation between Knudsen-and Torsion-Effusion Methods	8
	Effect of Orifice Dimensions on Equilibrium Pressure	9
CHAPTER III	EXPERIMENTAL	11
	Description of the Apparatus	11
	The Balance	11
	The Torsion-Effusion Assembly	14
	The Optical Lever System	21
	The Vacuum System	21
	The Heating Chamber	23
	The Furnace and Temperature Control and Measurement	23
	Calibrations	25
	Characteristics of the Effusion Cells	30
	Operational Procedures	30
CHAPTER IV	VAPOR PRESSURE AND THERMODYNAMIC PROPERTIES OF TETRAPHENYLTIN	34
	Literature Review	34
	Material	34
	Experimental Measurements	34
	Results	35

Comparison of Simultaneous Measurements via Torsion Recoil and Mass Effusion	Page 46
Error Analysis	49
Derived Thermodynamic Properties	49
Discussion	52
Summary	55
CHAPTER V VAPOR PRESSURE AND THERMODYNAMIC PROPERTIES OF HEXAPHENYLDITIN	
Literature Review	57
Material	57
Experimental Measurements	57
Results	58
Comparison of Simultaneous Measurements via Torsion Recoil and Mass Effusion	72
Error Analysis	72
Derived Thermodynamic Properties	72
Discussion and Conclusions	74
CHAPTER VI RECOMMENDATIONS FOR FUTURE WORK	76
BIBLIOGRAPHY	77

LIST OF TABLES

	Page
I Sample of Data of Torsional-Constant Calibration	28
II Measurement of the Torsional Constant	29
III Parameters of Effusion Cells	31
IV Knudsen-Effusion Data of Tetraphenyltin, Experiment No. 1	36
V Knudsen-Effusion Data of Tetraphenyltin, Experiment No. 2	37
VI Knudsen-Effusion Data of Tetraphenyltin, Experiment No. 3	38
VII Knudsen-Effusion Data of Tetraphenyltin, Experiment No. 7	39
VIII Torsion-Effusion Data of Tetraphenyltin, Experiment No. 7	40
IX Summary of Vapor-Pressure Data of Tetraphenyltin	47
X Knudsen-Effusion Data of Hexaphenylditin, Experiment No. 4	59
XI Knudsen-Effusion Data of Hexaphenylditin, Experiment No. 5	60
XII Torsion-Effusion Data of Hexaphenylditin, Experiment No. 5	61
XIII Knudsen-Effusion Data of Hexaphenylditin, Experiment No. 6	62
XIV Torsion Effusion Data of Hexaphenylditin, Experiment No. 6	63
XV Summary of Vapor-Pressure Data of Hexaphenylditin	69

LIST OF FIGURES

	Page
1. Schematic of Torsion-and Knudsen Effusion Apparatus	13
2. Schematic of the Torsion Assembly	16
3. Schematic of a Brass-Effusion Cell	19
4. Schematic of an Aluminum-Effusion Cell	20
5. Schematic of a Sand-Fluidized Bath	24
6. Sublimation Pressure of Tetraphenyltin by Knudsen Effusion, Experiment No. 1	41
7. Sublimation Pressure of Tetraphenyltin by Knudsen Effusion, Experiment No. 2	42
8. Sublimation Pressure of Tetraphenyltin by Knudsen Effusion, Experiment No. 3	43
9. Sublimation Pressure of Tetraphenyltin by Knudsen- and Torsion-Effusion, Experiment No. 7	44
10. Summary of Sublimation Data of Tetraphenyltin by Knudsen Effusion	45
11. Composite of Knudsen-Effusion Data of Tetraphenyltin	48
12. Comparison of the Vapor Pressure Data of Tetraphenyltin	53
13. Sublimation Pressure of Hexaphenylditin by Knudsen Effusion, Experiment No. 4	64
14. Sublimation Pressure of Hexaphenylditin by Knudsen- and Torsion-Effusion, Experiment No. 5	65
15. Sublimation Pressure of Hexaphenylditin by Knudsen- and Torsion-Effusion, Experiment No. 6	66
16. Summary of Sublimation Data of Hexaphenylditin by Knudsen Effusion	67
17. Summary of Sublimation Data of Hexaphenylditin by Torsion Effusion	68
18. Composite of Knudsen-Effusion Data of Hexaphenylditin	70
19. Composite of Torsion-Effusion Data of Hexaphenylditin	71

CHAPTER I

INTRODUCTION

Despite a notable increase in the number of organometallic compounds synthesized in recent years, there is a lack of reliable thermodynamic data for this class of compounds. This unsatisfactory state of affairs has been caused by the failure of conventional thermochemical techniques, when applied to such compounds. Recent developments of thermochemical techniques have assisted in obtaining precise data for a few organometallic compounds. However, the available data are still insufficient to allow calculations of the strengths of metal-to-carbon bonds in the majority of these compounds.

The thermochemical data required to calculate bond strengths and the wealth of information which can be gained from studies of their variations and deviations from expected trends in a given series of compounds, include the enthalpies of formation of such compounds and of their atomic and free radical constituents. It has been pointed out by Pauling¹ that the enthalpy of formation could be taken as a measure of the strength of bonds in a molecule. A common expression of the strength of a chemical bond is the "bond energy," which is derived from the enthalpy of formation of the compound, in its hypothetical ideal gas state, ΔH_f° (g). The enthalpy of formation of a compound, in its stable state at room temperature, can be determined from measurements of the heat of combustion, ΔH_c° . In the case of

compounds whose stable state, at room temperature, is the condensed state, the derived enthalpy of formation, from calorimetric measurements, is that of the condensed phase. However, the enthalpy of formation in the gaseous state can be determined by allowing for the enthalpy of vaporization, ΔH_v^0 , or the enthalpy of sublimation, ΔH_s^0 , according to:

$$\Delta H_f^0 (g) = \Delta H_f^0 (c) + \Delta H_v^0 \text{ (or } \Delta H_s^0) \quad (\text{I-1})$$

Since the enthalpies of vaporization and sublimation are measured above room temperature, variations of the molar heat capacity with temperature should be accounted for.

From the standard enthalpy of formation of the gaseous compound, it is possible to calculate the enthalpy change that accompanies the dissociation of the gaseous compound into its gaseous atoms and (or) free radicals. This enthalpy of atomization or fragmentation, ΔH_a^0 , which is the sum of the bond energies in a molecule:

$$\Delta H_a^0 = \sum E_b \quad (\text{I-2})$$

is related to the enthalpies of formation of the gaseous compound and its constituents according to:

$$\Delta H_a^0 = \sum \Delta H_f^0 (g, \text{ atoms or free radicals}) - \Delta H_f^0 (g, \text{ compound}) \quad (\text{I-3})$$

For a molecule of the type AB_n , containing only A-B bonds, it is reasonable to divide the enthalpy of atomization of the compound amongst the n bonds, (A-B), so that the average bond energy, $\bar{E} (A-B)$, is defined according to:²

$$\bar{E} (A-B) = \frac{1}{n} \Delta H_a^0 (AB_n, g) \quad (\text{I-4})$$

The average bond energies expressed as such do not bear a simple relation to bond dissociation energies and are not necessarily

numerically identical with them, on the contrary, the two measures often differ by substantial amounts. The widespread acceptance of \bar{E} values as an index of bond strength continues nonetheless, largely as a matter of expediency due to lack of more direct information.³

In this project, the sublimation behavior of tetraphenyltin, $\text{Sn}(\text{Ph})_4$, and hexaphenylditin, $\text{Sn}_2(\text{Ph})_6$, was investigated in the temperature ranges 406 to 461 K and 443 to 503 K, respectively. From the linear Clausius-Clapeyron relation:

$$\log_{10} P(\text{atm}) = - \frac{\Delta H_S^0}{2.303RT} + \frac{\Delta S_S^0}{2.303R} \quad (\text{I-5})$$

the enthalpies and entropies of sublimation, ΔH_S^0 and ΔS_S^0 , were calculated and utilized in evaluating the average bond energy, \bar{E} (Sn-Ph), in tetraphenyltin and the bond energy, E (Sn-Sn), in hexaphenylditin. The sublimation studies were performed using the simultaneous mass-effusion and torsion-recoil technique.

CHAPTER II

THEORY

The Knudsen-Effusion Method

The Knudsen-effusion method of determining vapor pressures is based upon the kinetic theory of dilute gases.⁴ According to the kinetic theory of gases, the weight of gas molecules, w , striking a container wall of area, A_0 , within a period of time, t , is directly proportional to the density, ρ , and the mean velocity, \bar{c} , of the gaseous molecules:

$$w/A_0 t = 1/4(\rho \bar{c}) \quad (\text{II-1})$$

From the ideal gas law, the density, ρ , is related to the pressure, P , temperature, T , and molecular weight, M , of the gas:

$$\rho = P M / R T \quad (\text{II-2})$$

Also from the kinetic theory of gases, the mean velocity, \bar{c} , is given by:

$$\bar{c} = (8RT/\pi M)^{1/2} \quad (\text{II-3})$$

One may substitute equations (II-2) and (II-3) into (II-1) to obtain a more useful relationship which after rearrangement, gives:

$$P_K = (w/A_0 t) (2 \pi RT/M)^{1/2} \quad (\text{II-4})$$

Equation (II-4) is the well known Knudsen-effusion relation⁵ where P_K is the Knudsen vapor pressure. From the Knudsen equation it is possible to calculate the vapor pressure of a substance by determining the rate of effusion through an orifice of known area,

assuming that the molecular weight of the effusing species is known. This method is useful for determining vapor pressures in the range of 10^{-2} to 10^{-6} Torr. There are four conditions which must be met before equation (II-4) is valid. These are:

- (1) the condensed and vapor phase must be in equilibrium;
- (2) the pressure of the cell enclosure into which the vapor is effusing must be negligible compared to the pressure of the vapor inside the cell;
- (3) there must be no collisions of vapor molecules within the orifice opening, i.e., there must be a laminar flow of molecules through the orifice;
- (4) there must be only a negligible fraction of molecules which collide with the orifice walls and return into the cell.

The first condition can be easily met by allowing the system sufficient time to equilibrate at a constant temperature. The second condition can be met by using a vacuum system which maintains a relatively low pressure outside the cell; a pressure of the order of 10^{-6} Torr should be satisfactory. The third condition places an upper limit on the vapor pressure for which this method can be applied with reasonable accuracy; since the higher the pressure the greater will be the frequency of collisions.

The fourth condition is very difficult to obtain. A perfect orifice is both perfectly round and infinitely thin. In practice, an orifice has a finite thickness, and this will allow a significant number of molecules to strike the walls of the orifice and rebound into the cell. Fortunately, however, a correction factor has been

developed by Clausing.^{6,7} The Clausing factor, W_o , is related to the ratio of thickness to radius of the orifice, l/r , according to:

$$W_o = 1/\sqrt{1 + 0.5(l/r)} \quad (\text{II-5})$$

for $0 < l/r < 1.5$, and

$$W_o = \sqrt{1 + 0.4(l/r)} / \sqrt{1 + 0.95(l/r) + 0.15(l/r)^2} \quad (\text{II-6})$$

for $(l/r) > 1.5$. The Clausing factor, W_o , represents the probability that a molecule, once it has entered the orifice, will strike the orifice walls and rebound into the cell. A tabulation of Clausing factors which makes it possible to determine the correction factor for an orifice of known l/r ratio is available.⁸ Incorporation of the Clausing factor into the Knudsen equation results in the following modified Knudsen equation:

$$P_K = (w/A_o t W_o) (2\pi RT/M)^{1/2} \quad (\text{II-7})$$

Thus from measurements of temperature and the rate of weight loss through an orifice of known area and thickness, the vapor pressure of vapor species of known molecular weight can be calculated from equation (II-7).

The Torsion-Effusion Method

Torsional recoil is another method of determining vapor pressures directly by a simple dynamic technique. The torsion method utilizes the recoil force of vapor molecules as they effuse through the orifices of a cell, with two orifices situated so that a torque is produced on the cell as the vapor effuses. With the cell suspended by a fine filament the torque generated by the effusing vapor will be counterbalanced by a restoring torque from the suspension

filament. This will result in an angular displacement of the suspension system. Mayer⁹ and Volmer¹⁰ were the first to utilize torsional recoil in an effusion experiment to measure vapor pressures directly.

The recoil force exerted by the effusing species is related to the vapor pressure by the following relation:

$$P = 2F/A_0 \quad (\text{II-8})$$

where P is the vapor pressure, F is the recoil force of the effusing molecules, and A_0 is the cross sectional area of the orifices. The force of the effusing species is related to the torque exerted on the cell according to:

$$T_r = Fd \quad (\text{II-9})$$

where T_r is the torque and d is the moment arm, i.e., the distance from the center of the orifice to the axis of rotation. Since there are two antiparallel orifices in an effusing cell, the resultant torques are additive:

$$T_r = F_1d_1 + F_2d_2 \quad (\text{II-10})$$

The "restoring torque" in the filament, T_w , which counterbalances the torque, T_r , produced by the effusing molecules is proportional to the angular displacement, θ :

$$T_w = T_r = \zeta \theta \quad (\text{II-11})$$

where ζ is the torsion constant of the filament. Thus the vapor pressure of the effusing sample can be obtained directly from measurements of the angular displacement of a suspension system with known torsion constant of its filament, by use of cells of known orifice characteristics. Substitution of equations (II-10)

and (II-11) into equation (II-8) yields:

$$P_{\tau} = 2 \tau \theta / (A_1 d_1 f_1 + A_2 d_2 f_2) \quad (\text{II-12})$$

The new variable, f_i , in equation (II-12) represents a correction factor analogous to the Clausing factor in the Knudsen-effusion equation. This factor represents the ratio of the recoil force produced from effusion through an orifice of finite thickness to that expected for an orifice with an infinitesimal thickness. The f -factor, referred to also as the "pressure factor," has been reported by Searcy and Freeman¹¹ and more recently by Schulz and Searcy¹², for orifices of different ℓ/r ratios.

Correlation between Knudsen-and Torsion-Effusion Methods

Vapor pressure measurements by torsion effusion and Knudsen effusion can be performed simultaneously, since a torsion effusion cell is a modification of a conventional Knudsen cell. Vapor pressures measured by the torsion effusion as indicated by equation (II-12) do not require any knowledge of the molecular weight of the vapor species. On the other hand, such information is essential for vapor pressure calculation from mass-effusion measurements according to equation (II-7). Simultaneous measurements of torsional recoil and mass effusion can be used to determine the average molecular weight of the vapor species. Substitution for the Knudsen pressure, P_K , in equation (II-7) by the torsion-effusion pressure, P_{τ} , from equation (II-12), yields an average molecular weight, M^* , expressed by:

$$M^* = 2\pi RT(w/P_o t A_o W_o)^2 \quad (\text{II-13})$$

This average molecular weight, if different from the molecular weight of the condensed phase, is related to the molecular weights of the individual constituents of a vapor mixture, resulting from polymerization and/or dissociation, by the following expression:¹¹

$$M^* = \frac{\sum m_i M_i^{-1/2}}{\sum m_i}^{-1} \quad (\text{II-14})$$

where m_i is the mass fraction of vapor species i and M_i is the molecular weight of that species. From a knowledge of the average molecular weight, calculated in this manner, it is possible to establish whether vaporization or sublimation processes are simple, or involve decomposition or polymerization of the compound, in the vapor phase. If there is a discrepancy between the assumed molecular weight and the calculated average molecular weight one may speculate the nature of the decomposition or polymerization process.

Effects of Orifice Dimensions on Equilibrium Pressure

The vapor pressure measured by the Knudsen-effusion cell is not an equilibrium vapor pressure of the system because of the continuous effusion of the vapor through the orifice. It is expected that the smaller the orifice area the smaller the deviation of the measured vapor pressure from the equilibrium vapor pressure. A relationship which relates the measured Knudsen vapor pressure to the equilibrium vapor pressure is:^{13,14}

$$P_{eq} = P_K (1 + A_o W_o / \alpha_c s) \quad (\text{II-15})$$

where s is the sample's surface area assumed to be equal to the

cross sectional area of the cell, α_c is the condensation coefficient*, P_{eq} is the equilibrium pressure, P_K is the measured Knudsen pressure, and A_0 and W_0 have been previously defined. Equation (II-15) may be rearranged to a more useful form:

$$1/P_K = (1/P_{eq}) \bar{l} + (W_0 A_0 / \alpha_c s) \bar{l} \quad (II-16)$$

a series of Knudsen experiments with cells of different orifice areas could be undertaken which would measure different vapor pressures at one temperature. A plot of $1/P_K$, at one temperature, vs. the orifice area is linear and extrapolation to zero orifice area would result in an intercept at $1/P_{eq}$. The slope of the line would represent the value $W_0 / \alpha_c s P_{eq}$. It would be possible, therefore, to obtain the equilibrium vapor pressure and assess the value of the condensation coefficient of the compound under investigation, since the Clausing factor and the cross section area of the cell are known. Here, it is assumed that the sample area is equivalent to that of the cell cross section. This assumption is practiced in these assessments, although its validity is questioned.

*Condensation coefficient is the fraction of sample molecules which condense upon collision with the sample surface.

CHAPTER III

EXPERIMENTAL

Description of the Apparatus

The apparatus used to measure the mass effusion and torsion recoil simultaneously is essentially a composite of a balance, a torsion-effusion assembly, an optical-lever system, a heating chamber, a furnace and temperature control-and measurement-system. A general schematic of the apparatus is shown in Figure 1.

The Balance

The balance is an Ainsworth Semimicro recording balance, type RV-AU-1. It is capable of detecting weight changes as small as 0.1 milligram by a variable inductance transducer and bridge circuit. As the beam of the balance deflects, due to weight change, the transducer senses the magnitude of the deflection. The electronic signal from the transducer causes a response in the bridge circuit, which is part of a servomechanism connected to a potentiometer shaft. The position of the pen mounted on the potentiometer becomes a measure of weight. The potentiometer can respond to weight changes as large as 10 milligrams, without exceeding the limit of the slidewire. When the weight changes exceed 10 milligrams a relay system with a motor and various cams and levers adds or subtracts weights in 10 milligram increments to bring the pen back on scale. The reproducibility of the balance is ± 0.03 milligram, the sensitivity is 0.1

KEY TO FIGURE 1

Schematic of Torsion-and Knudsen-Effusion Apparatus

1. Vacuum recording balance
2. Balance stand
3. Brass extension tube
4. Brass evacuation line
5. Liquid-nitrogen trap
6. Oil diffusion pump
7. Thermocouple gauge
8. Ionization gauge
9. Pyrex tube
10. Mechanical pump
11. Roughing valve
12. Main gate valve
13. Fore-line vacuum valve

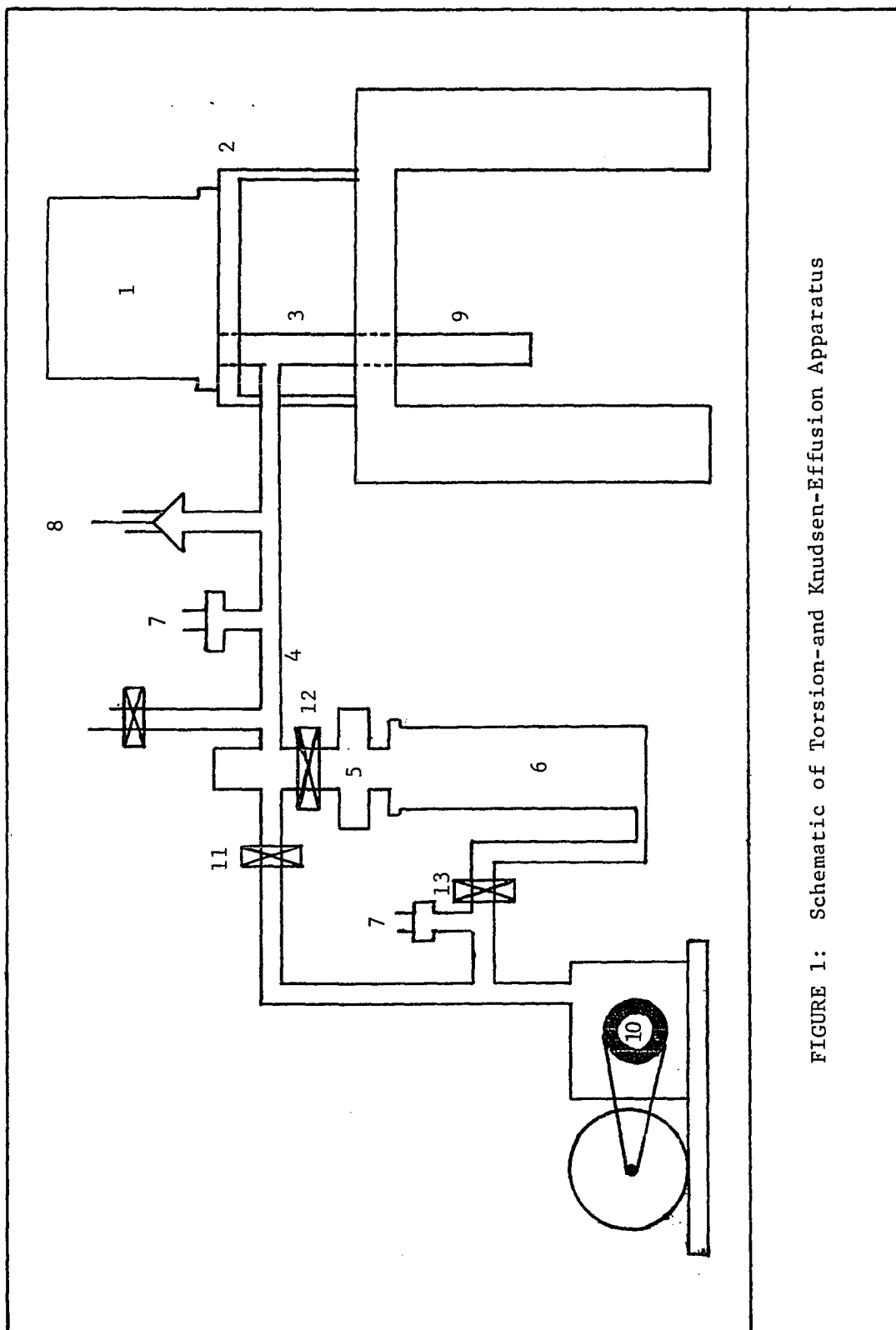


FIGURE 1: Schematic of Torsion- and Knudsen-Effusion Apparatus

milligram per scale division of chart paper, and the chart paper can be read to within 0.03 milligram. The balance is mounted on a base plate and enclosed within a pyrex bell jar. It is connected to the vacuum system and weighing chamber via a hole in the base plate beneath the left stirrup.

The Torsion-Effusion Assembly

The torsion-effusion assembly, shown in Figure 2, consists of, in the order from top to bottom, a stool and connector, a torsion fiber, a mirror and damping-disc assembly, and an effusion cell and its suspension extension. The entire assembly is suspended from the left beam of the balance.

The stool and connector

The left pan of the balance has a hole drilled through its center and a circular groove milled around the hole. An aluminum stool shaped as a tripod, which sets on three equispaced brass pins, is positioned on the pan, guided by the circular groove. The center of the stool has inserted into it a rotatable drum to which is fastened a small pin vise. This arrangement permits rotational and lateral alignment of the torsion assembly. The pin vise extends through the holes in the pan and base plate, along with the filament, into a brass tube.

The torsion filament

The above mentioned vise is used to hold one end of the

KEY TO FIGURE 2

Schematic of the Torsion Assembly

1. Stool and connector on balance pan
2. Torsion fiber
3. Mirror
4. Damping disc
5. Effusion cell
6. Glass window
7. Scale
8. Thermocouple

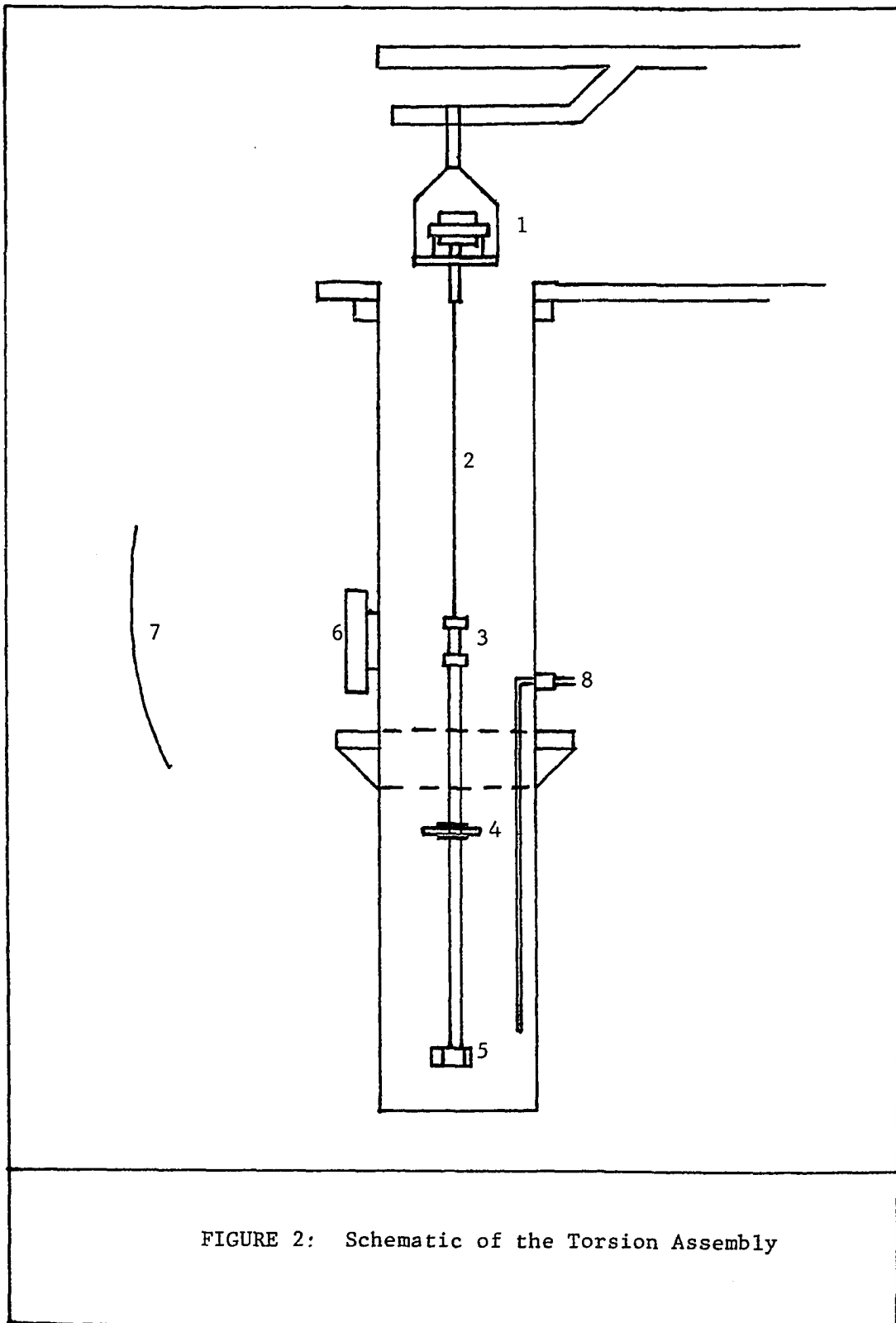


FIGURE 2: Schematic of the Torsion Assembly

torsion filament. The filament is an annealed high purity tungsten wire 0.0015 inch in diameter and exactly 14 inches long between the tips of the two vises which hold it. The lower vise supports the mirror holder and connects the filament to the suspension tube and the cell.

The mirror, connector, tube, and damper

An aluminum rod with a notched position for the mirror is fastened to the lower vise. The mirror is positioned so that its front surface coincides with the axis of rotation of the torsion system. The mirror is a front-surface galvanometer type, 0.5 inch in diameter and concave with a radius of curvature of one meter. The bottom vise with the mirror and its supporting aluminum rod is joined to the suspension extension tube by means of a tungsten pin which extends through two matching holes, drilled into the tube and aluminum rod. The extension tube is of stainless steel, 0.125 inch in diameter, 0.005 inch wall thickness, and approximately 15 inches long. The lower end of the tube is joined firmly to a dovetail of brass or aluminum with the aid of a tungsten pin. The dovetail connects the effusion cell to the system via a carefully matched keyway in the cell body.

An aluminum disc 1.5 inches in diameter and 0.125 inch thick is fastened at about 6 inches below the mirror with the aid of a set screw. This disc allows for magnetic damping of the rotational oscillations of the torsion assembly. A horseshoe electromagnet powered by a Heathkit D.C. power supply (Model IP-12) is used for

this purpose.

The effusion cell

Two different types of cells were used. The first set of cells was machined from $5/8$ inch diameter brass rod. Each cell is $1\ 1/2$ inches long, $3/8$ inch inside diameter, and $1/2$ inch outside diameter, except for the middle portion of $1/2$ inch length, which was an outside diameter of $5/8$ inch. The dovetail-matching keyway is machined carefully into this thick middle portion. The two ends of the cell are fitted with two degrees tapered brass plugs. Two orifices were drilled on opposite sides of the cell, $5/16$ inch from each end. Before the orifices were drilled, the walls in the immediate vicinity of the orifices were milled, so that reasonably thin orifices were obtained. A sketch of this type of cell is shown in Figure 3.

The second type of cell is machined from aluminum rod. The cell consists of a central portion $1/2$ inch long, $5/8$ inch outside diameter, and $3/8$ inch inside diameter and two end portions $3/4$ inch long, $3/8$ inch inside diameter and $1/2$ inch outside diameter. The central portion joins the two end portions through two degrees matching tapers. Each outer portion is cylindrical with one closed end and a tapered open end. An orifice is drilled into each of the two outer portions, $1/8$ inch from the closed end. The cell wall is also milled down so that the orifice thickness is as small as possible. Figure 4 shows a schematic of this type.

When a cell of either type is assembled, scribed marks are

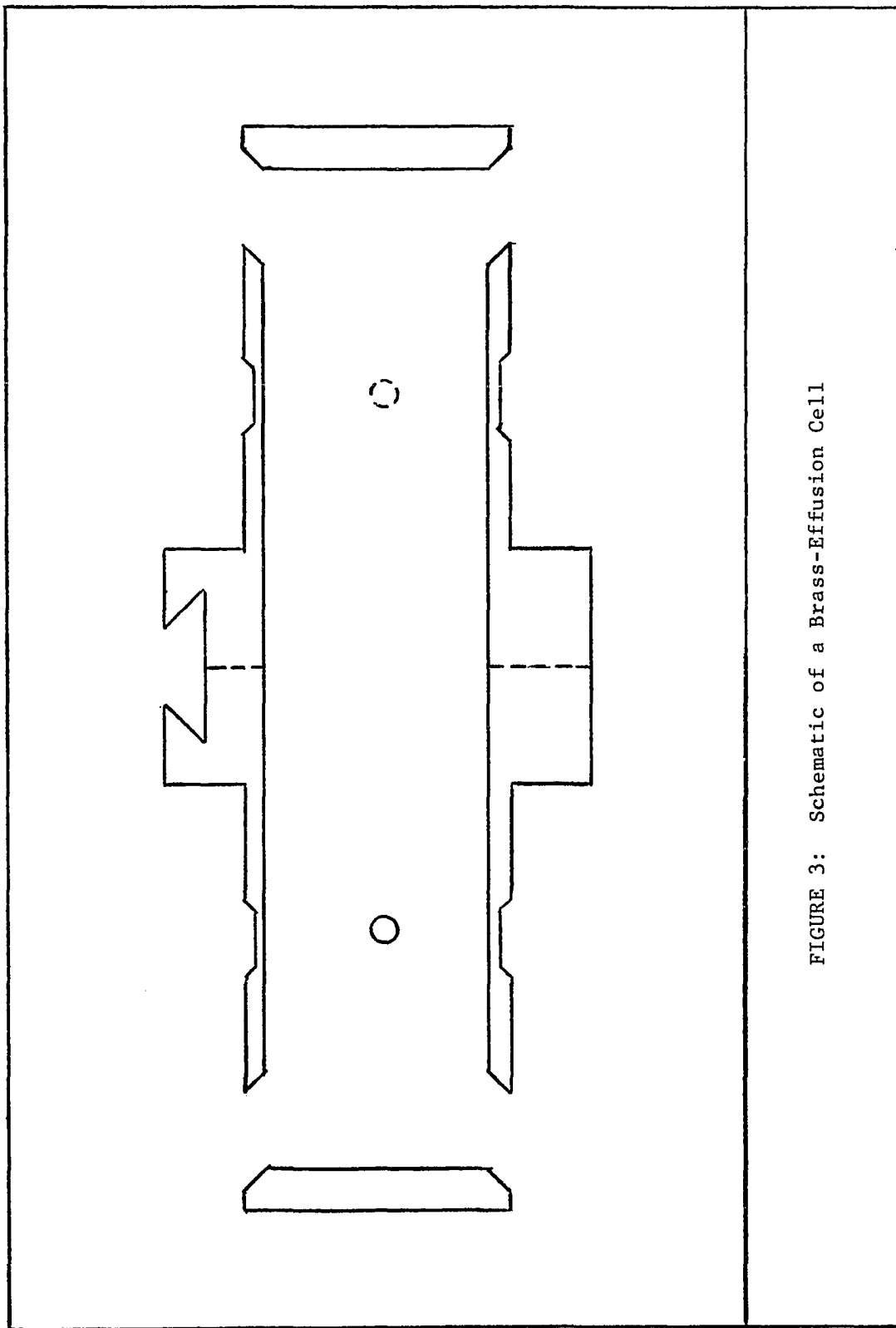


FIGURE 3: Schematic of a Brass-Effusion Cell

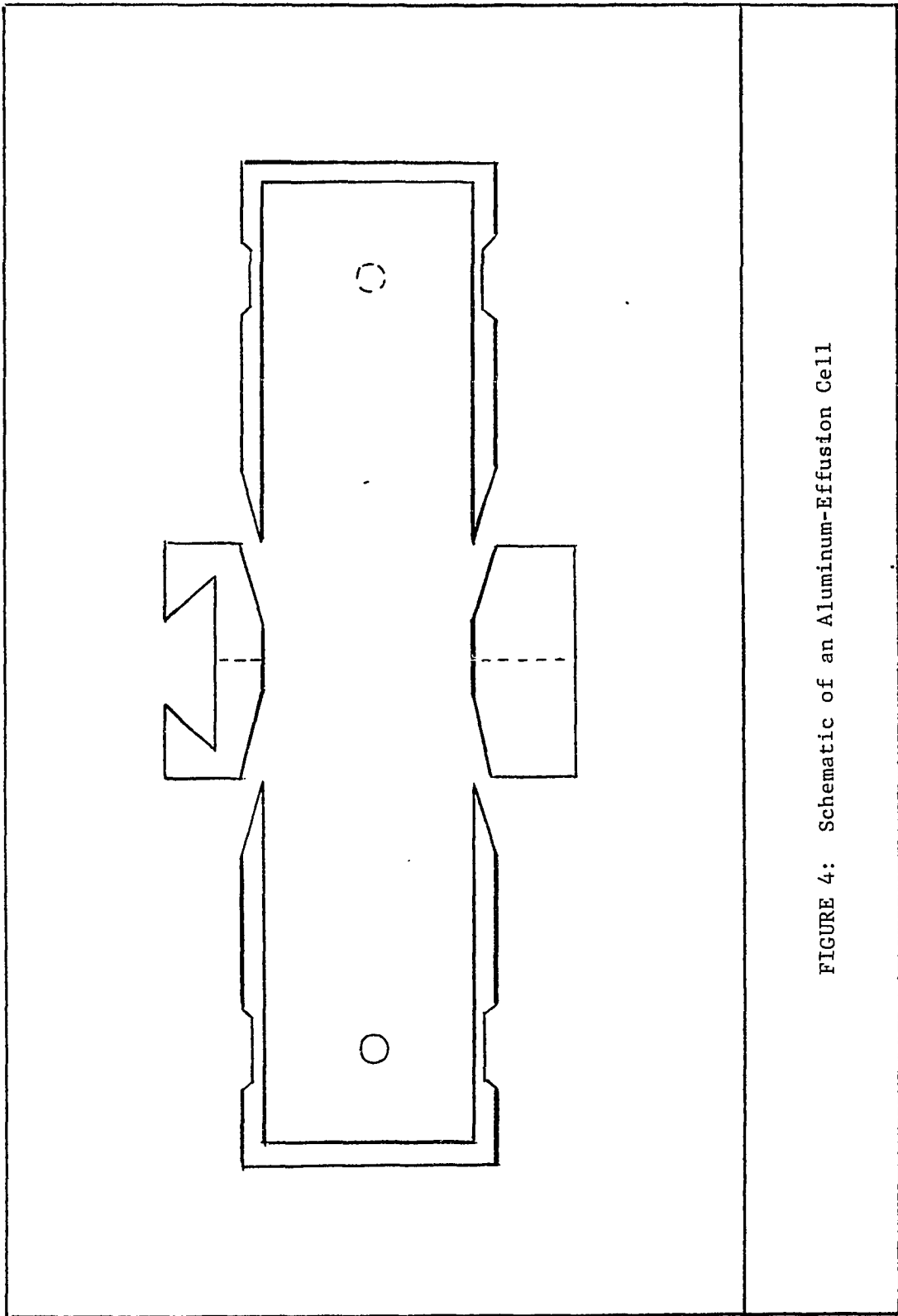


FIGURE 4: Schematic of an Aluminum-Effusion Cell

used to align the orifices properly on opposite sides of the cell. The aluminum and brass cells each have their own dovetail fitting of the same material attached to the stainless steel tube of the torsion system.

The Optical Lever System

The mirror of the torsion assembly is a component of the optical lever system which is used to determine the deflection due to torsional recoil caused by vapor effusion. A collimated light source and a flexible scale are the other components. A beam of light from the light source, after reflection at the mirror surface, falls on the mounted scale which forms an arc of a circle 36 inches in radius, with the mirror as a center. The scale is graduated in two hundredths of an inch.

From equation (II-12) the angular deflection is required to determine the vapor pressure. The angular deflection in radians is equal to the linear deflection on the scale in inches, divided by twice the radius of curvature of the arc according to the optical lever principle.

The Vacuum System

The balance is connected to the vacuum system through a brass tube, two inches in diameter and seventeen inches long. The tube, which encloses the torsion assembly, is connected to the base plate of the balance by an O-ring flange. Two ports are fitted into the brass tube. The top port connects the balance to the main vacuum

system. Connections to the system are via a vacuum coupling on the balance side and a glass pipe flange with a kovar seal on the pump side. A side arm tube, fitted with a vacuum stopcock, forms a T-joint with this glass tube. The stopcock opens to the atmosphere and allows bleeding of dry air into the balance, when desired. The lower port of the extension brass tube is fitted with a glass window at the same level as the mirror on the torsion assembly. This port permits the incident beam of light to be reflected by the mirror and onto the scale.

The vacuum system consists of an oil diffusion pump (National Research Corporation Series HS2-300) and a mechanical pump (Precision Scientific Company Model D-150). At the intake of the diffusion pump there is a Chevron baffle cryogenic trap to prevent contamination of the balance with diffusion oil. A two inch gate valve isolates the diffusion pump from the balance. An all copper-tubing manifold connects the oil diffusion pump outlet to the mechanical pump. It is conventional with respect to a by-pass line for roughing, and vacuum valves in the foreline, and roughing line and for air bleeding.

The pressure in the system is measured by two thermocouple gauges (NRC Equipment Corporation, type 521) one placed between the balance and the diffusion pump and the other between the diffusion pump and the mechanical pump. An ionization gauge (NRC Equipment Corporation, type 538-P) is used to measure high vacuum and is located close to the balance between the balance and the diffusion pump. The gauges are controlled by the Thermocouple and Emission

Regulated Ion Gauge Console (NRC type 720).

The Heating Chamber

The flanged lower end of the brass extension tube connects the balance to the heating chamber. The heating chamber is a pyrex tube provided with an O-ring flange at its open end. It is shaped like a test tube. It is 15 3/4 inches long, 2 5/8 inches inside diameter, and 4mm wall thickness. This tube encloses the suspended cell.

The Furnace and Temperature Control and Measurement

The furnace and temperature control

The sample is heated by a Tecam sand fluidized bath, type SBS4 produced by the British Aluminum Company, and is illustrated in Figure 5. The bath is 18 inches high and 7 1/2 inches inside diameter. The fluid portion of the bath is 9 inches deep. The fluid used in the bath is a fine-grained sand. Air is blown through the bottom of the bath which causes the sand to appear as a gently boiling liquid. The air supply is controlled by a pressure regulator fitted with a filter to prevent contamination of the sand. The flow rate is controlled by adjustment of the pressure regulator. Reproducibility of the flow rate is observed by a float flowmeter. The cover of the bath is made of aluminum. The top of the cover is fastened down by means of two clips, and has two holes drilled through it, one for the heating chamber and the other for a thermostat. Due to vibrations caused by the passage of air through

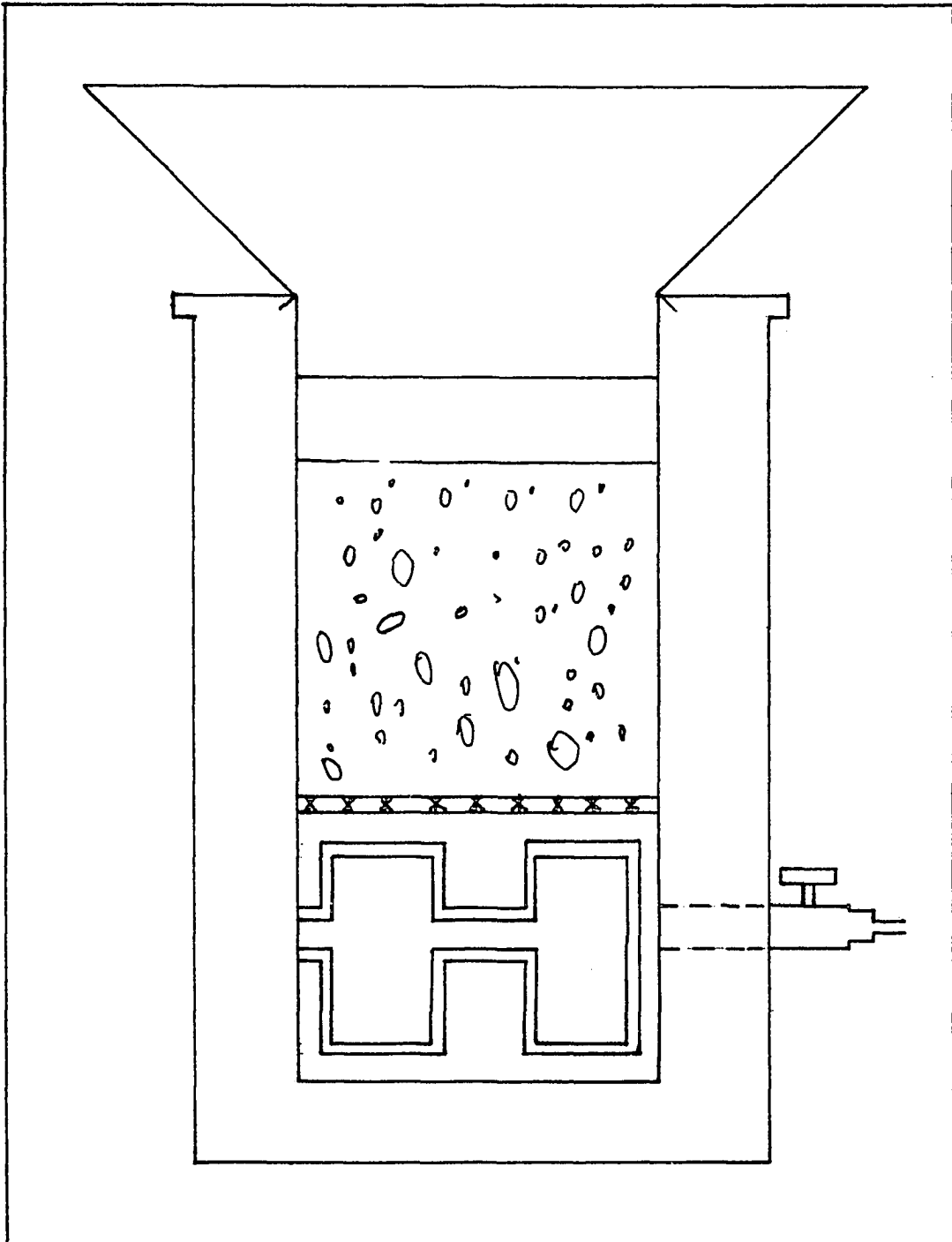


FIGURE 5: Schematic of a Sand-Fluidized Bath

the sand, a brass cylinder, 9 inches high and 3 inches in diameter, closed at one end, surrounded the heating chamber, inside the bath, without direct contact between the brass cylinder and the heating chamber. The top of the bath cover, with the aid of two lead weights, holds the brass cylinder in place so that vibration effects are eliminated.

Power is supplied to the bath from 110/120 line voltage through a powerstat variable transformer. The bath has two heating coils, one coil sufficient for moderate temperatures from 100-250 C and an additional coil used for higher temperatures (up to 600 C) and for fast heating. The temperature is regulated by transistorized relay and mercury thermoregulator.

Temperature measurement

The temperature is measured by a chromel-alumel thermocouple. The thermocouple is inserted inside the heating chamber through the brass extension tube. A vacuum feed-through is used to lead the thermocouple terminals outside the system. The thermocouple hangs free, and at a fixed position of approximately 5mm above the top of the cell, inside the heating chamber. The thermocouple output is measured by a portable potentiometer (Honeywell model 2745).

Calibrations

Calibrations of the thermocouples

Since the measuring thermocouple must be outside the cell, it was necessary to calibrate the measuring thermocouple with a ref-

erence thermocouple placed inside the cell. The reference thermocouple is of the same composition as the measuring thermocouple; it was calibrated at the freezing points of lead, zinc, aluminum, and copper, and a reference junction temperature of 0 C. The relationship of the emf produced by the reference thermocouple to the temperature is:

$$T(K) = A + B(mv)_r \quad (III-1)$$

where $A = 275.38_6$ and $B = 24.22_2$. The intercomparison of the measuring thermocouple with the reference thermocouple is expressed in a linear relation as follows:

$$(mv)_r = A_1 + B_1(mv)_{ex} \quad (III-2)$$

where the constants A_1 and B_1 are 0.1598 and 1.0065, respectively.

By substitution of equation (III-1) into equation (III-2) one obtains:

$$T(K) = (A + BA_1) + BB_1(mv)_{ex} \quad (III-3)$$

Equation (III-3) is further simplified into:

$$T(K) = A_2 + B_2(mv)_{ex} \quad (III-4)$$

where $A_2 = 279.25_7$ and $B_2 = 24.37_8$. This equation relates the temperature inside the cell to the emf of the measuring thermocouple.

The propagated error in these constants, A_2 and B_2 and the estimated precision of measurement of the thermocouple output yield an estimated error of 0.25 K which is consistent with the average deviation of the temperature over the period of mass effusion measurement at a given temperature setting.

Calibration of the torsion filament

The torsion constant, ζ , of the filament was determined from

measurements of the period of oscillation of a torsional pendulum incorporating the torsion assembly and a cylindrical ring replacing the effusion cell. The ring is mounted on a cross bar at the lower end of the torsion assembly. The torsional constant is related to the moment of inertia of the cylindrical ring, I , and periods of oscillation according to:

$$\tau = 4\pi^2 I / (T_1^2 - T_2^2) \quad (\text{III-5})$$

where T_1 and T_2 are the periods of oscillation with and without the ring on the cross bar respectively. The rings and cross bars are made of aluminum and brass. The moment of inertia of the rings is related to its dimensions according to:¹⁵

$$I = \frac{m}{8}(D_1^2 + D_2^2) \quad (\text{III-6})$$

where m is the mass of the ring, D_1 is the inside diameter and D_2 is the outside diameter. In a calibration experiment, the number of oscillations during a given time are counted by an electric counter activated by a relay circuit incorporating a photocell. The optical lever system is utilized in the torsion constant calibration where the light beam reflected from the mirror is intercepted by the photocell twice for each oscillation and eventually the counter registers two counts for one oscillation. The data of a typical calibration measurement are shown in Table I. The measured torsional constants of the filaments used in this work are listed in Table II.

The values of the torsion constant, for the same filament, have been found to vary from experiment to experiment. The maximum fluctuation was 2.8%, or what corresponds to approximately 0.03 dyne cm rad^{-1} . The propagated error in the value of τ arising from the

TABLE I

Sample of Data of Torsional-Constant Calibration

Pendulum of Suspension System with Aluminum Crossbar

Pt. No.	Counts	Time (sec)	Oscillations	Sec/Period
1	100	973.2	50	19.464
2	102	993.1	51	19.472
3	104	1013.1	52	19.483
4	106	1033.8	53	19.506
5	108	1053.0	54	19.500
6	110	1072.9	55	19.507
Average				19.489

Pendulum of Suspension System with Aluminum Crossbar and Ring

Pt. No.	Counts	Time (sec)	Oscillations	Sec/Period
1	48	1584.6	24	66.025
2	50	1651.6	25	66.064
3	52	1718.7	26	66.104
4	54	1789.4	27	66.274
5	56	1856.4	28	66.300
6	58	1923.6	29	66.331
Average				66.183

TABLE II

Measurement of the Torsional Constant

Parameters of the Ring of the Torsion Pendulum

Parameter	Aluminum	Brass
Inside Diameter (cm)	5.398	5.392
Outside Diameter (cm)	5.716	5.720
Mass (g)	11.9604	39.4653
Moment of Inertia (g cm ²)	92.411	304.830

Calibration Measurements of Tungsten Wire of 0.0015 Inches Diameter

Experiment	Ring Material	Time per Oscillation (sec)		Torsional Constant (dyn cm rad ⁻¹) τ
		With Crossbar T_2	With Crossbar & Ring T_1	
4	Brass	26.497	117.589	0.9169
4	Aluminum	19.518	66.119	0.9142
5 ^b	Aluminum	19.584	66.362	0.9074
5 ^a , 6 ^b	Aluminum	19.489	66.183	0.9119
6 ^a , 7 ^b	Aluminum	19.697	67.033	0.8885
7 ^a	Aluminum	19.672	66.417	0.9066

- a) Measurement after experiment
- b) Measurement before experiment

uncertainties, in the individual errors in mass, radii, and time estimated from the precision of their respective measurements, is $\pm 1.05\%$ or what corresponds to approximately $0.01 \text{ dyne cm rad}^{-1}$. This value is consistent with results of repeated measurements of the torsional constant of a given filament before and after an experiment.

Characteristics of the Effusion Cells

A traveller microscope which could be read to $\pm 0.0025 \text{ mm}$ was used to measure the orifice diameters and moment arms. For orifice-diameter measurements, the cell was positioned in eight different orientations and the average of these measurements was considered. The uncertainty of the orifice diameter is $\pm 0.43\%$, and the uncertainty of the moment arm is $\pm 0.2\%$. The corresponding error in the orifice area is $\pm 0.86\%$. The thickness was measured using a vernier caliper which reads to the nearest 0.0005 inch . The ratio of the thickness to the radius of the orifice was used to determine the Clausing factor for Knudsen-effusion data considerations and the Pressure factor for torsion-recoil calculations. The characteristics of both sets of cells are tabulated in Table III.

Operational Procedure

Prior to a typical experiment the entire torsion assembly, except for the cell, must be weighed. This step is necessary to check the weight of deposit on the torsion assembly and to correct for it, if necessary. Next the cell is loaded with approximately $0.6\text{-}0.8 \text{ g}$ of sample and then attached to the torsion assembly using a dovetail

TABLE III

Parameters of Effusion Cells

Cell No.	Dia. of orifices (cm x 10 ²)	Areas (cm ² x 10 ³)	Moment arm (cm x 10)	Clausing Factor	Pressure Factor	
Set I: Brass Cells ^a						
I-2	1	7.47	4.38	9.148	0.88093	0.9157
	2	7.75	4.72	9.957	0.88486	0.9187
I-3	1	8.91	6.23	8.997	0.89822	0.9289
	2	9.28	6.76	9.086	0.90175	0.9316
I-4	1	11.54	10.46	8.918	0.91958	0.9447
	2	11.41	10.22	9.007	0.91872	0.9441
Set II: Aluminum Cells ^b						
II-1	1	8.233	5.32	15.825	0.78470	0.83652
	2	8.214	5.30	15.440	0.78440	0.83626
II-2	1	9.863	7.64	15.621	0.81308	0.86085
	2	9.794	7.53	16.063	0.81210	0.86003
II-3	1	12.146	11.59	16.052	0.84268	0.88540
	2	12.042	11.39	15.820	0.84125	0.88424

a) All orifice lengths were 1.016×10^{-2} cm.

b) All orifice lengths were 2.286×10^{-2} cm.

connection, and a second weighing is made of the torsion assembly including the loaded cell. Proper adjustments of the torsion assembly orientation are made to insure that the reflected light beam is intercepted on the scale, at a point which permits covering the deflection range within its ends. The entire system is then sealed, the furnace is put into position, and the mechanical pump is started to rough down the system to a pressure of 10^{-2} Torr. At this point the oil diffusion pump is put into operation. After a stable pressure of 10^{-5} to 10^{-6} Torr has been attained, the zero point of the optical lever system should be read and recorded. The bath is heated to approximately 110 C for two hours, after which the temperature is raised gradually to a point just above the upper temperature limit desired in the sublimation study of a given compound. At this point the temperature is lowered to any desired setting for vapor pressure measurements.

During a vapor-pressure determination there must be as nearly a constant temperature as possible. The system requires anywhere from two to four hours to achieve stability. When a constant temperature is obtained the weight loss recording is started. Deflection and temperature measurements are read every fifteen minutes during the time required for a reasonable weight loss at a constant temperature. In a typical experiment the temperatures are selected at random. At the beginning of each day a new zero point of the optical lever system is read and the vacuum in the system is checked. When an entire experiment is completed the system is allowed to cool completely to room temperature. The diffusion pump

is turned off and allowed to cool, and the balance is isolated from the vacuum pumps. The bleeding valve is opened, and the balance is brought slowly to atmospheric pressure. When the furnace and heating chamber are removed the cell is disconnected, and, finally, the suspension system is weighed to determine the amount of sample, if any, deposited on the torsion assembly during the experiment.

CHAPTER IV

VAPOR PRESSURE AND THERMODYNAMIC PROPERTIES OF TETRAPHENYLTIN

Literature Review

Only one investigation of the temperature dependence of the vapor pressure of tetraphenyltin has been carried out prior to this work. Carson, et. al.¹⁶ measured the vapor pressure of tetraphenyltin at a narrow temperature range, 25-42.5 C. Their measurements were carried out by means of the Knudsen-effusion method and a flow proportional counter to assay the tritium of the effusate of a tritium-labelled sample of tetraphenyltin. Their data led to an enthalpy of sublimation, $\Delta H_{\text{sub}}^{\circ} = 15.85 \pm 0.3 \text{ kcal mole}^{-1}$ and a vapor pressure of $(6.32 \pm 0.3) \times 10^{-9}$ mm of Hg at 298 K.

Material

Tetraphenyltin, used in this work, was a recrystallized sample of the commercially available compound from Alpha Inorganics, Inc. Recrystallization was from benzene solution, which gave a purified sample whose melting point is 225-227.5 C, compared with the literature melting point of 224-225 C.¹⁷

Experimental Measurements

Vapor pressure measurements were performed by the apparatus and according to the procedure described in Chapter III. Prior to

effusion-rate or torsion-deflection measurements the loaded cell was heated gradually to about 185 C. After a weight loss of approximately 20 mg. the temperature was readjusted to the desired temperature for an experimental point. The temperatures, for each of a succession of measurements, were selected at random. The total weight loss was in the range of 350-380 mg. The residual pressure was maintained during an experimental period within 10^{-5} to 10^{-6} Torr.

Results

The saturated vapor pressure in equilibrium with solid tetraphenyltin was determined from measurements of the rate of effusion in three experiments, with brass cells of different parameters, and from simultaneous measurements of the rate of effusion and torsional recoil in a fourth experiment, using an aluminum cell. Calculations of the vapor pressure were carried out by means of equation (II-7) for the effusion-rate data and equation (II-12) for the torsion data. The molecular weight of the monomer, $427.117 \text{ g mole}^{-1}$, was assumed for equation (II-7). Clausius-Clapeyron equations,

$$\log_{10} P = A + B/T \quad (\text{IV-1})$$

with parameters established by least-squares analyses were obtained, using an IBM 1620 Computer. The experimental data, the computed vapor pressures, and Clausius-Clapeyron equations are tabulated in Tables IV to VIII and presented graphically in Figures 6 to 10.

The second-law enthalpies and entropies of sublimation obtained

TABLE IV

Knudsen-Effusion Data of Tetraphenyltin, Experiment¹ No. 1^a

Pt. No.	Weight Loss w (g x 10 ³)	Time t (min)	Temperature T (K)	Pressure P (atm)	10 ⁴ /T (K ⁻¹)	-log P
1	13.25	75.0	439.7	8.393 x 10 ⁻⁶	22.742	5.076
2	0.41	165.0	397.5	1.122 x 10 ⁻⁷	25.160	6.950
3	0.41	105.0	402.4	1.774 x 10 ⁻⁷	24.853	6.751
4	5.64	185.0	422.3	1.419 x 10 ⁻⁶	23.678	5.848
5	8.19	120.0	430.6	3.208 x 10 ⁻⁶	23.225	5.494
6	9.12	95.0	434.2	4.532 x 10 ⁻⁶	23.029	5.344
7	10.63	20.0	454.6	2.567 x 10 ⁻⁵	21.996	4.591
8	24.89	30.0	458.2	4.024 x 10 ⁻⁵	21.823	4.395
9	20.59	70.0	446.6	1.408 x 10 ⁻⁵	22.390	4.851

$$\log_{10} P \text{ (atm)} = (12.263 \pm 0.186) - (7644 \pm 80) T^{-1}$$

a) Effective orifice area: $8.03 \times 10^{-3} \text{ cm}^2$.

TABLE V

Knudsen-Effusion Data of Tetraphenyltin, Experiment No. 2^a

Pt. No.	Weight Loss w (g x 10 ⁻³)	Time t (min)	Temperature T (K)	Pressure P (atm)	10 ⁴ /T (K ⁻¹)	-log P
1	0.94	120.0	406.9	2.467 x 10 ⁻⁷	24.577	6.608
2	1.10	10.0	433.6	3.552 x 10 ⁻⁶	23.061	5.449
3	22.67	30.0	453.7	2.503 x 10 ⁻⁵	22.042	4.602
4	1.90	70.0	419.0	8.620 x 10 ⁻⁷	23.869	6.064
5	5.52	95.0	427.7	1.868 x 10 ⁻⁶	23.382	5.729
6	4.54	25.0	439.0	5.910 x 10 ⁻⁶	22.777	5.228
7	14.82	35.0	448.1	1.394 x 10 ⁻⁵	22.319	4.856
8	1.30	30.0	424.2	1.387 x 10 ⁻⁶	23.575	5.858

$$\log_{10} P \text{ (atm)} = (12.737 \pm 0.264) - (7882 \pm 114) T^{-1}$$

a) Effective orifice area: $1.170 \times 10^{-2} \text{ cm}^2$.

TABLE VI

Knudsen-Effusion Data of Tetraphenyltin, Experiment No. 3^a

Pt. No.	Weight Loss w (g x 10 ³)	Time t (min)	Temperature T (K)	Pressure P (atm)	10 ⁴ / T (K ⁻¹)	-log P
1	0.68	30.0	413.8	4.406 x 10 ⁻⁷	24.168	6.356
2	1.06	430.0	393.8	4.664 x 10 ⁻⁸	25.394	7.331
3	0.93	215.0	399.1	8.243 x 10 ⁻⁸	25.058	7.084
4	1.80	220.0	403.8	1.573 x 10 ⁻⁷	24.764	6.803
5	0.68	50.0	408.9	2.628 x 10 ⁻⁷	24.468	6.580
6	0.94	45.0	413.9	4.062 x 10 ⁻⁷	24.160	6.391
7	1.99	50.0	418.4	7.779 x 10 ⁻⁷	23.902	6.109
8	1.36	15.0	428.6	1.792 x 10 ⁻⁶	23.331	5.747
9	4.54	25.0	433.8	3.619 x 10 ⁻⁶	23.050	5.441
10	20.51	50.0	443.1	8.263 x 10 ⁻⁶	22.571	5.083
11	27.06	45.0	448.1	1.218 x 10 ⁻⁵	22.315	4.914
12	22.10	25.0	453.3	1.801 x 10 ⁻⁵	22.060	4.744

$$\log_{10} P \text{ (atm)} = (12.579 \pm 0.213) - (7837 \pm 88) T^{-1}$$

a) Effective orifice area: $1.901 \times 10^{-2} \text{ cm}^2$.

TABLE VII

Knudsen-Effusion Data of Tetraphenyltin, Experiment No. 7^a

Pt. No.	Weight Loss w (g x 10 ³)	Time t (min)	Temperature T (K)	Pressure P (atm)	10 ⁴ /T (K ⁻¹)	-log P
1	2.77	40.0	433.4	3.365 x 10 ⁻⁶	23.072	5.502
2	1.62	50.0	423.9	1.344 x 10 ⁻⁶	23.588	5.837
3	3.61	90.0	427.8	1.970 x 10 ⁻⁶	23.373	5.742
4	5.01	40.0	440.0	6.215 x 10 ⁻⁶	22.727	5.241
5	10.27	57.5	442.9	8.076 x 10 ⁻⁶	22.580	5.086
6	9.59	32.5	447.8	1.253 x 10 ⁻⁵	22.324	4.865
7	5.53	20.0	446.7	1.276 x 10 ⁻⁵	22.386	4.894
8	4.01	15.0	446.6	1.233 x 10 ⁻⁵	22.391	4.909
9	18.47	40.0	453.8	2.148 x 10 ⁻⁵	22.034	4.668
10	22.76	27.5	461.2	3.882 x 10 ⁻⁵	21.682	4.411

$$\log_{10} P \text{ (atm)} = (12.591 \pm 0.436) - (7829 \pm 193) T^{-1}$$

a) Effective orifice area: $8.33 \times 10^{-3} \text{ cm}^2$.

TABLE VIII

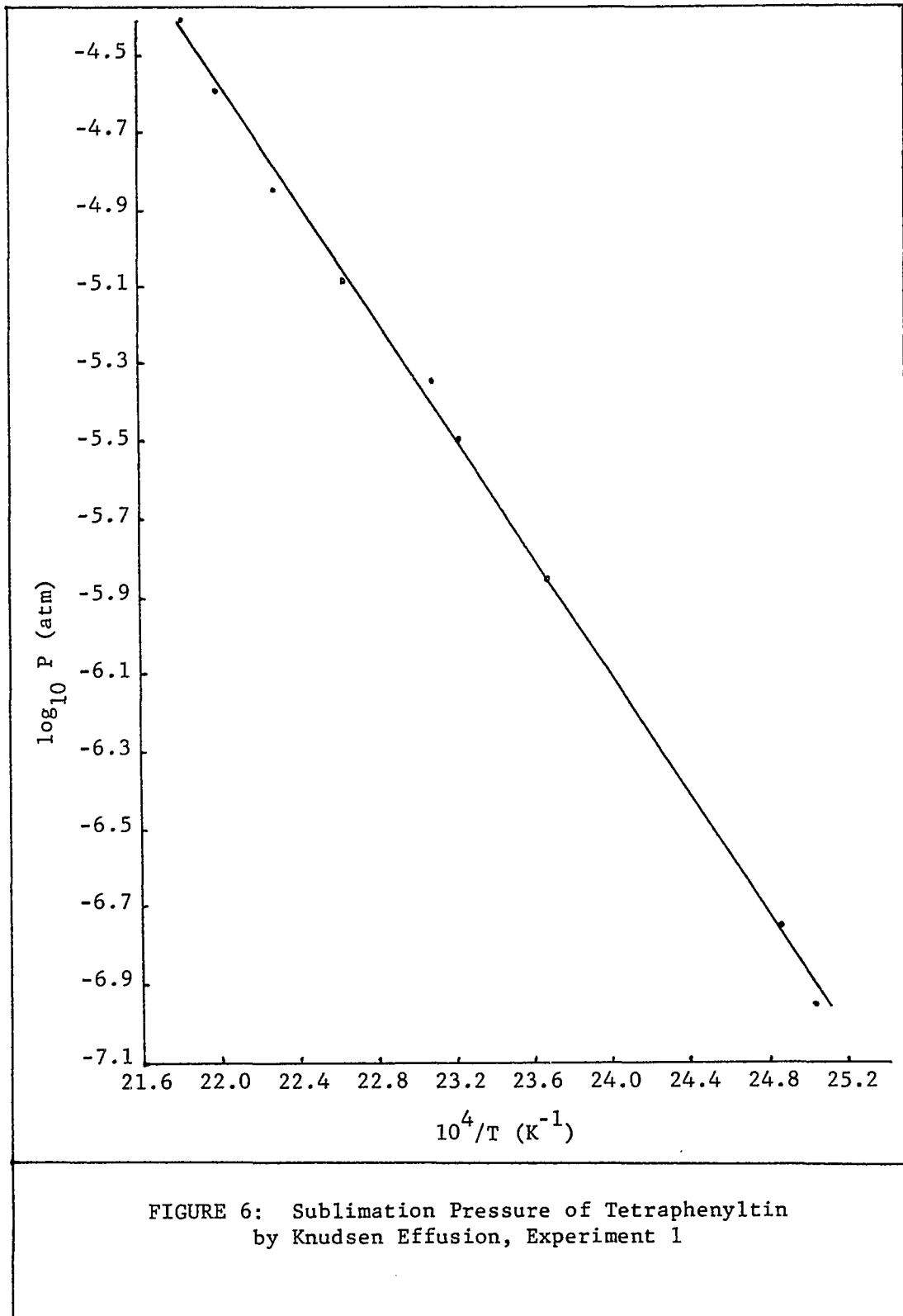
Torsion-Effusion Data of Tetraphenyltin, Experiment No. 7^a

Pt. No.	Deflection S (inch)	Temperature T (K)	Pressure P (atm)	$10^4/T$ (K ⁻¹)	-log P
1	12.32	453.5	2.182×10^{-5}	22.049	4.661
2	2.13	433.4	3.773×10^{-6}	23.072	5.423
3	1.09	427.8	1.931×10^{-6}	23.373	5.714
4	4.27	440.0	7.564×10^{-6}	22.726	5.121
5	5.83	442.9	1.033×10^{-5}	22.580	4.986
6	7.63	446.7	1.352×10^{-5}	22.385	4.869
7	13.55	453.7	2.400×10^{-5}	22.040	4.620

$$\log_{10} P \text{ (atm)} = (12.942 \pm 0.753) - (7963 \pm 33) T^{-1}$$

a) Effective orifice area x moment arm: $1.389 \times 10^{-2} \text{ cm}^3$.

Torsion constant, ζ : $0.8976 \text{ dyn cm rad}^{-1}$



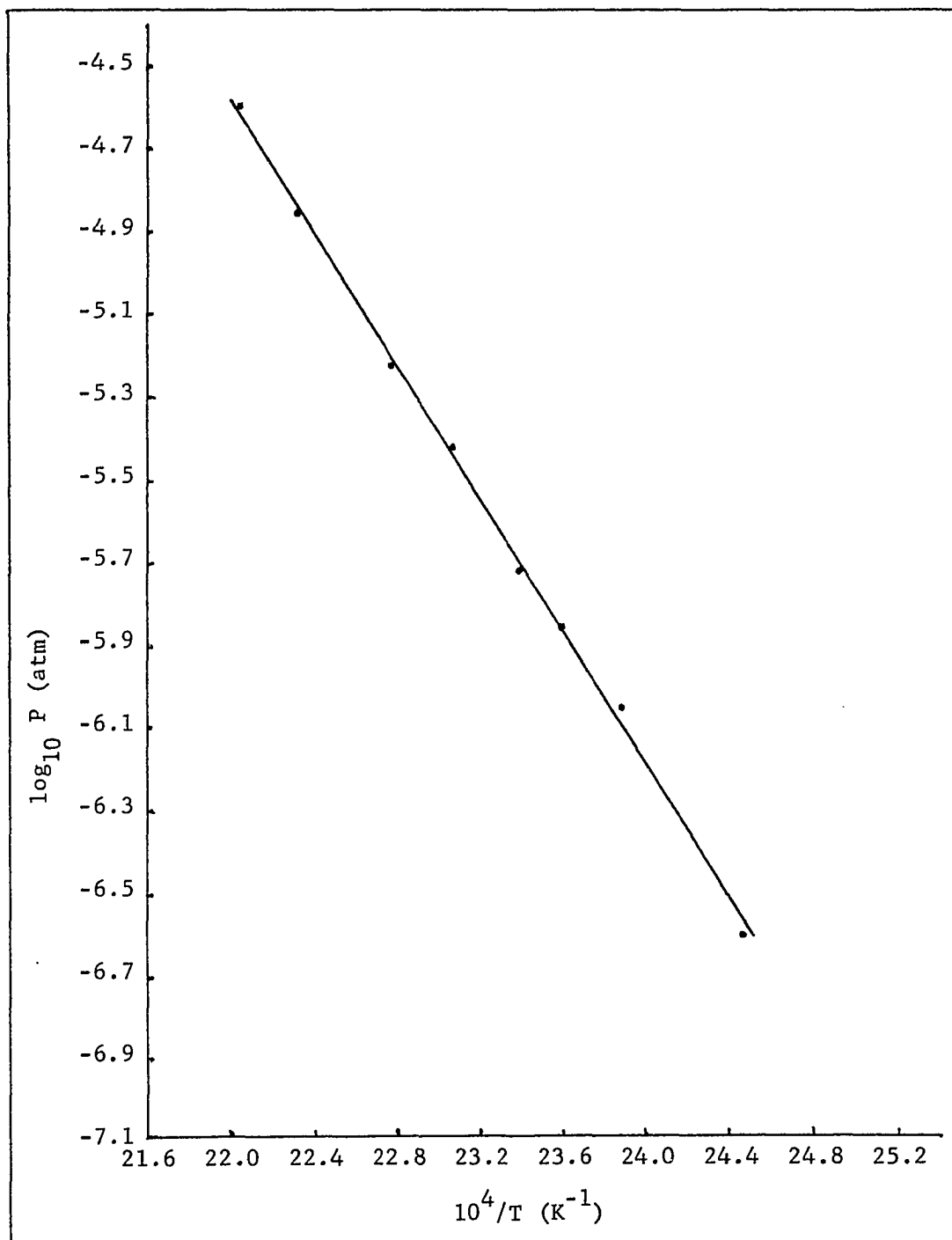
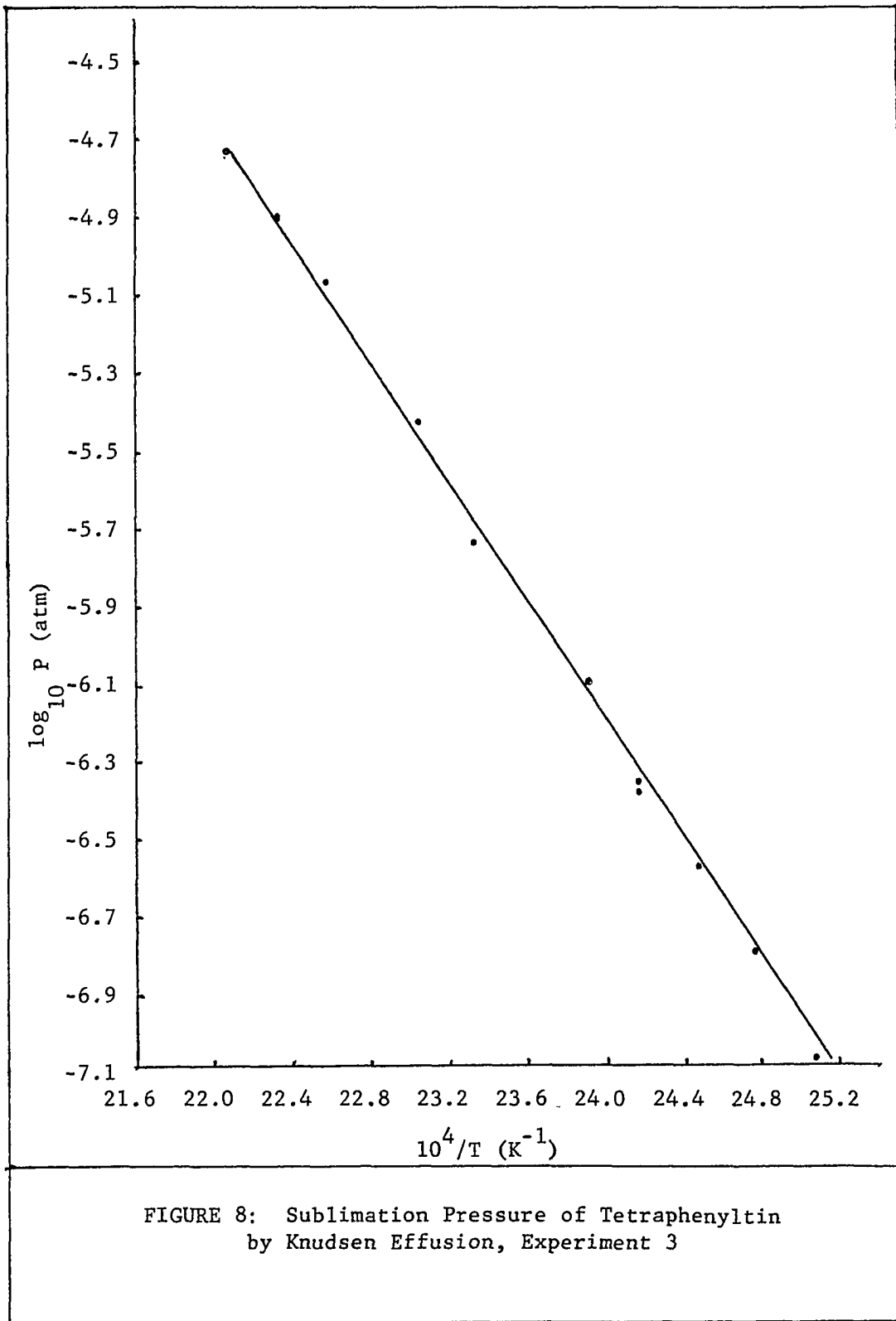


FIGURE 7: Sublimation Pressure of Tetraphenyltin
by Knudsen Effusion, Experiment 2



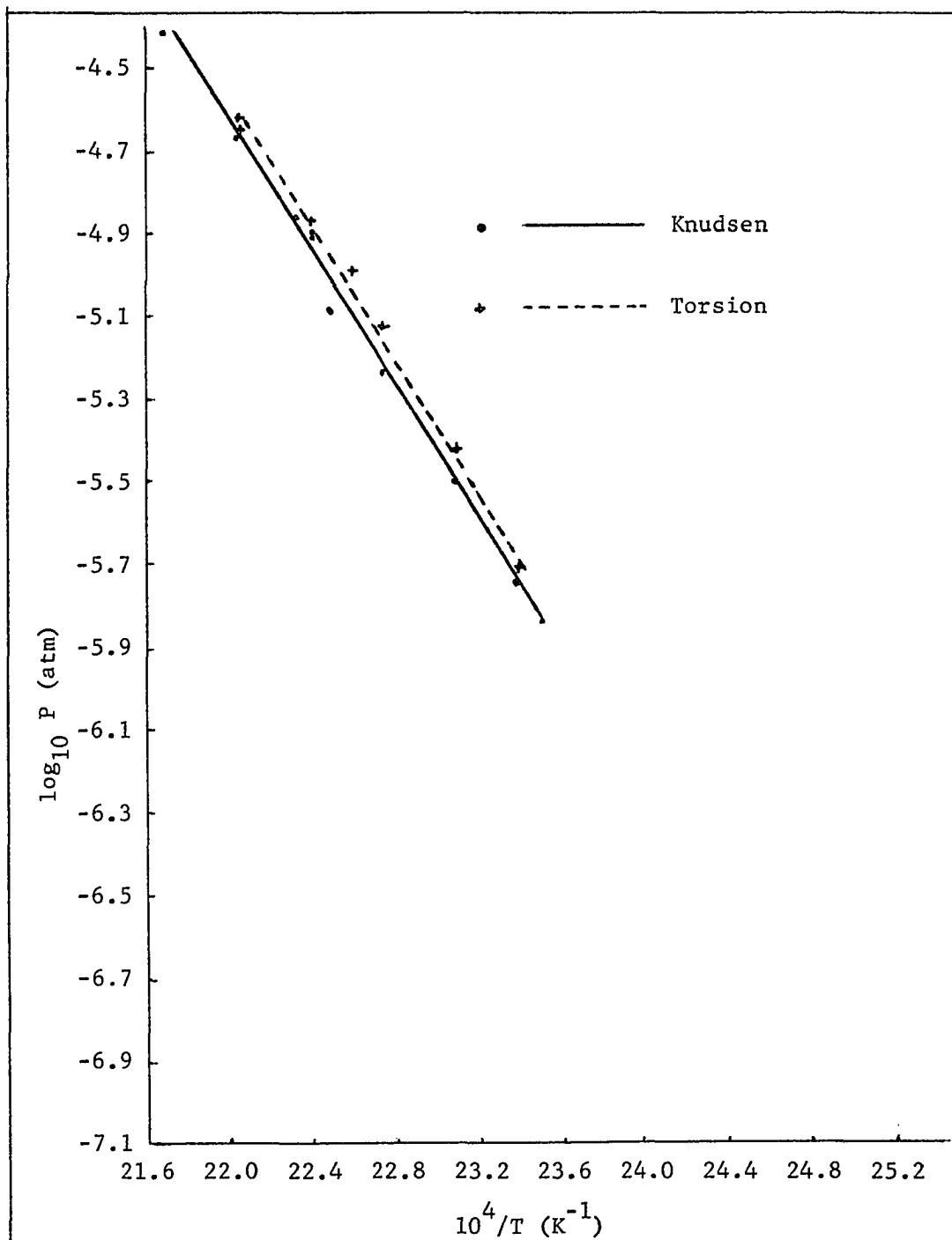
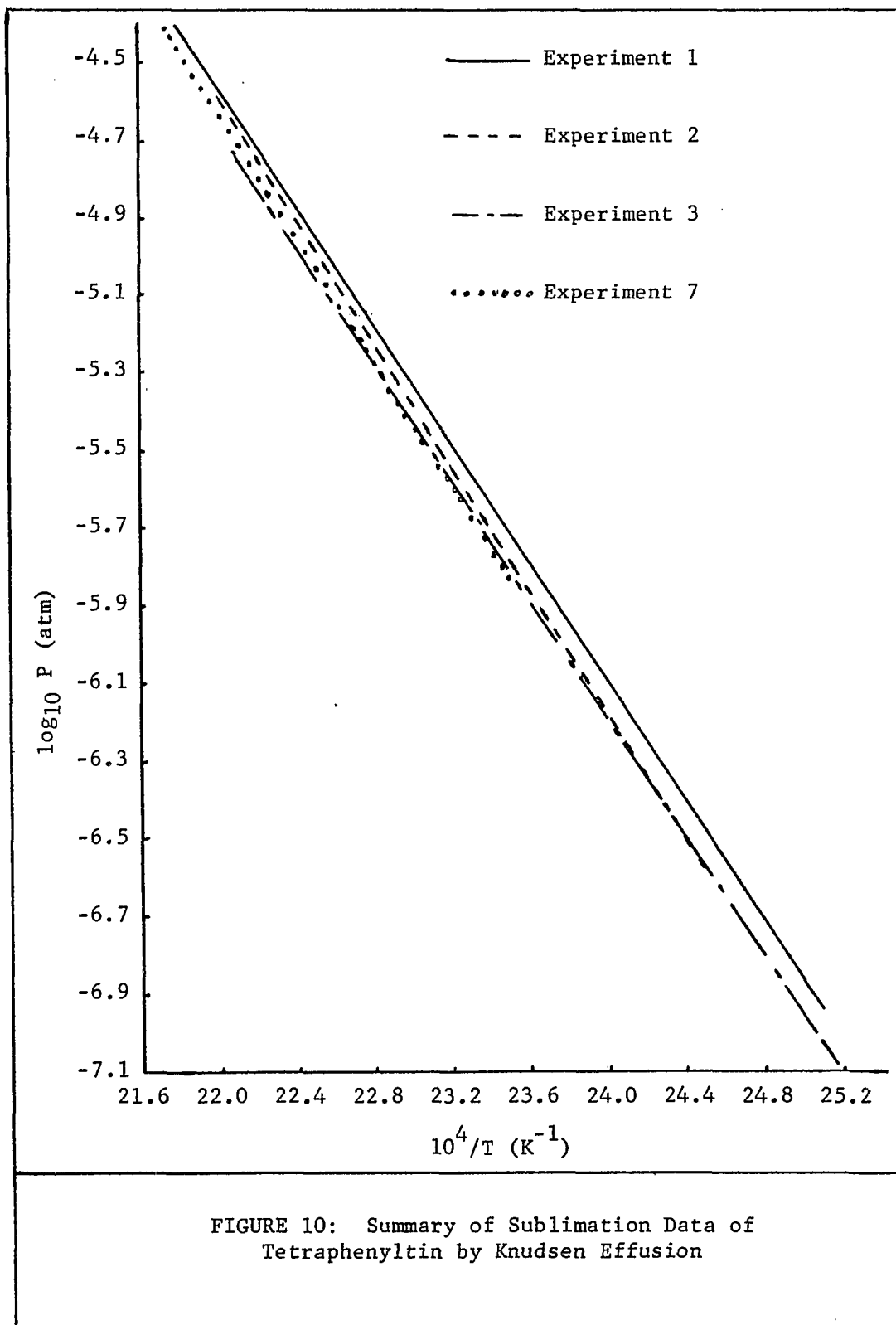


FIGURE 9: Sublimation Pressure of Tetraphenyltin by Knudsen- and Torsion-Effusion, Experiment 7



from the above treatment are summarized in Table IX. Also listed in this table are the values of $\log P$ and the standard deviations at the median temperature of 433 K. A composite least-squares analysis of all points of $\log P_K$ vs. T^{-1} in experiments 1, 2, 3, and 7 was performed. The results indicate that experiment 1 does not belong to the same set as do the other experiments. This is obvious by inspection of Table IX and from the successive rejection of points with the largest residual. The rejected points include all points of this experiment. Thus it is suggested that experiments 2, 3, and 7 are more reliable, but one has no meaningful criterion for such a decision. In the absence of a definitive criterion the composite results, listed in Table IX and presented in Figure 11, are accepted for the present.

Comparison of Simultaneous Measurements Via Torsion-Recoil and Mass Effusion

Inspection of Table IX and Figure 9 shows that the torsion pressure is higher than the Knudsen pressure of experiment 7. At the median temperature, 433 K, the ratio of P_T/P_K is 1.15. This lack of agreement between P_T and P_K may be attributed to two factors: 1) the torsion pressure is too large because of the effusate which returns preferentially to the same side of the cell;¹⁸ 2) dissociative sublimation into species of smaller molecular weights.

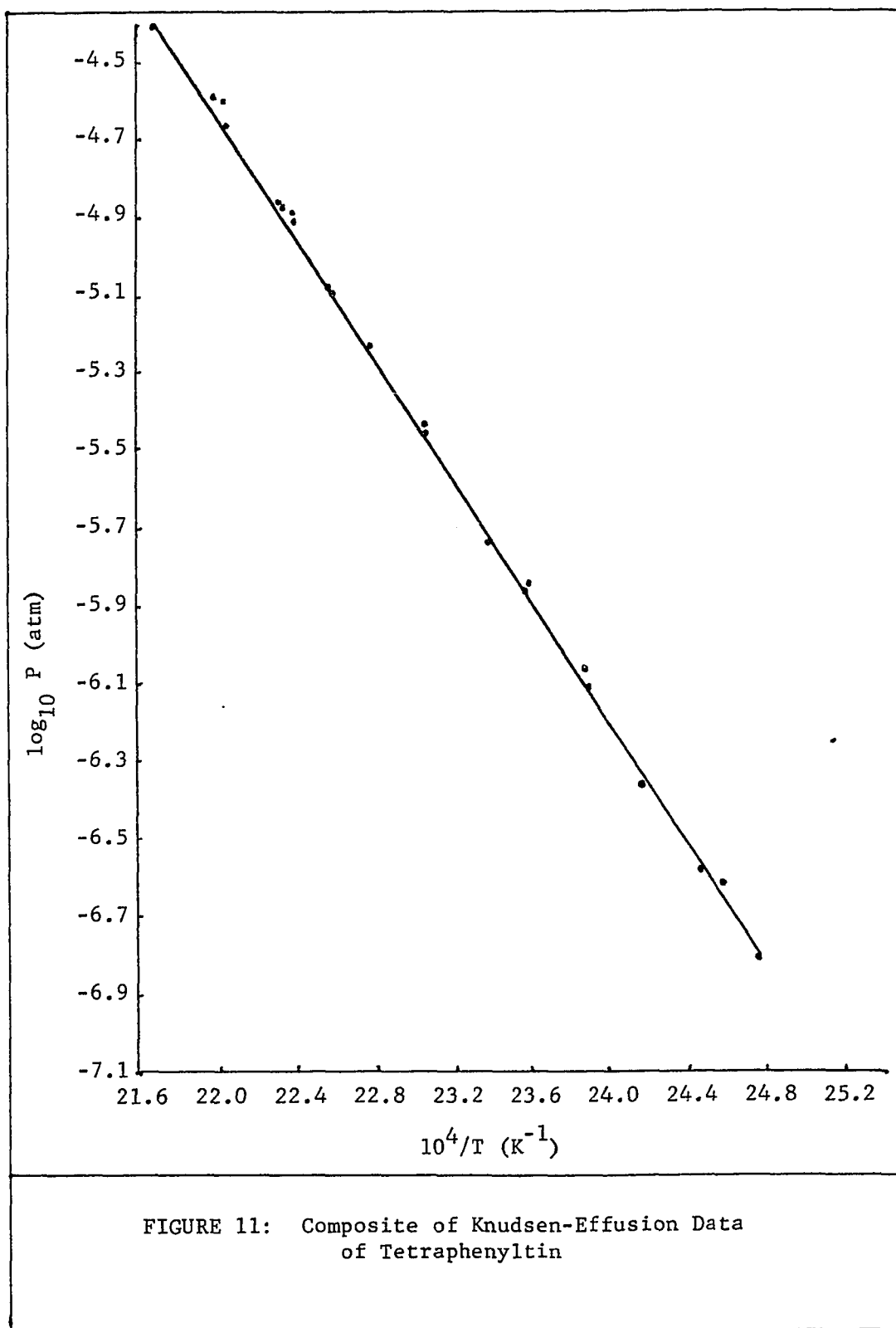
There have been several investigations^{11,19-21} in which the two measurements were simultaneous and $P_T > P_K$ even when the identity of the vapor species is well established as monomeric. The ratio

TABLE IX

Summary of Vapor-Pressure Data of Tetraphenyltin^a

Experiment	ΔH_T° (kcal mole ⁻¹)	ΔS_T° (eu)	$\log P_T$	P_T (atm)
1 Knudsen	35.0 ±0.04	56.1 ±0.8	-5.387	4.105 x 10 ⁻⁶
2 Knudsen	36.1 ±0.05	58.3 ±1.2	-5.467	3.415 x 10 ⁻⁶
3 Knudsen	35.9 ±0.04	57.6 ±1.0	-5.520	3.018 x 10 ⁻⁶
7 Knudsen	35.8 ±0.09	57.6 ±2.0	-5.490	3.093 x 10 ⁻⁶
2,3,7 Knudsen	36.1 ±0.08	58.3 ±2.0	-5.477	3.334 x 10 ⁻⁶
7 Torsion	36.4 ±0.01	59.2 ±3.4	-5.448	3.568 x 10 ⁻⁶

a) $\bar{T} = 433$ K



of P_{γ}/P_K of the reported cases range between 1.05 to 1.17. Dissociative sublimation in the present study may be ruled out on the basis of the equivalence of the melting points of the original pure sample, 225-227.5 C, the residue in the cell, 225-227 C, and the condensed effusate, 226-227 C. Further support was also established by similarity of the infra red spectra of the above and their agreement with the reported spectra.²²

Error Analysis

When measuring the Knudsen-effusion vapor pressure there is uncertainty in the following values: the weight loss, area of the orifice, time, and temperature. The propagated error in the Knudsen vapor pressure based on the uncertainties in these measurements is of a value of $\pm 3.5\%$ at lower pressures and $\pm 2.5\%$ for medium and high range vapor pressures.

When measuring the torsion-effusion vapor pressure there is uncertainty in the following values: the filament constant, the torsional deflection, the areas of the orifices, and the moment arm of the cells. These uncertainties lead to a propagated error in the torsion vapor pressure of $\pm 4.9\%$. The corresponding errors in the calculated vapor pressures from the least-squares treatment are $\pm 4.4\%$ for P_K and $\pm 6.8\%$ for P_{γ} .

Derived Thermodynamic Properties

To calculate the thermodynamic properties of gaseous tetraphenyltin from the measurements associated with sublimation of

tetraphenyltin the following additional data were employed.

Enthalpy of formation of SnPh₄ (s)

The heat of combustion of tetraphenyltin at 298 K was measured by Pope and Skinner²³ to be $-3177.7 \pm 0.8 \text{ kcal mole}^{-1}$. For the enthalpy of formation of SnPh₄ (s) they calculated the value $\Delta H_f^{\circ} (\text{SnPh}_4, \text{s}, 298 \text{ K}) = 98.5 \pm 0.9 \text{ kcal mole}^{-1}$, based on the combustion data.

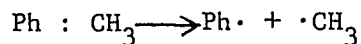
Enthalpy of formation of SnPh₄ (g)

The enthalpy of formation of gaseous tetraphenyltin is calculated from that of the solid and from the enthalpy of sublimation, $\Delta H_s^{\circ} = 36.1 \pm 0.1 \text{ kcal mole}^{-1}$, to be $136.5 \pm 1.0 \text{ kcal mole}^{-1}$. This value takes into account a correction of $2.0 \text{ kcal mole}^{-1}$ representing the difference between the enthalpy of sublimation at the median temperature of 433 K and the reference temperature of 298 K. Pope and Skinner reported a value of $114.3 \pm 1.0 \text{ kcal mole}^{-1}$ based on the heat of sublimation of $15.8 \pm 0.3 \text{ kcal mole}^{-1}$ reported by Carson et. al.¹⁶

Enthalpy of formation of the phenyl radical

The enthalpy of formation of a free radical is either measured directly from the enthalpy of a reaction in which the radical is formed or indirectly by measuring the enthalpy of formation of a compound containing the radical of interest, and the bond dissociation energies of compounds including the radical. In the case of

the phenyl radical the bond energy for the dissociation process of toluene:



has been obtained by Kandel²⁴ as, $E(\text{Ph}-\text{CH}_3) = 91 \text{ kcal mole}^{-1}$. From the enthalpy of formation of gaseous toluene, $\Delta H_f^\circ(\text{PhCH}_3, \text{g}) = 11.95 \text{ kcal mole}^{-1}$ and that of the methyl free radical, $\Delta H_f^\circ(\cdot\text{CH}_3, \text{g}) = 32 \text{ kcal mole}^{-1}$, the enthalpy of formation of the phenyl radical is found to be, $\Delta H_f^\circ(\cdot\text{Ph}, \text{g}) = 71 \pm 3 \text{ kcal mole}^{-1}$, according to

$$E(\text{Ph}-\text{CH}_3) = \Delta H_f^\circ(\cdot\text{Ph}, \text{g}) + \Delta H_f^\circ(\cdot\text{CH}_3, \text{g}) - \Delta H_f^\circ(\text{PhCH}_3, \text{g}) \quad (\text{IV-2})$$

Thus,

$$\Delta H_f^\circ(\cdot\text{Ph}, \text{g}) = 71.0 \text{ kcal mole}^{-1}$$

The uncertainty in $E(\text{R}-\text{X})$ calculated from $\Delta H_f^\circ(\text{R}, \text{g})$ and $\Delta H_f^\circ(\text{RX}, \text{g})$ is within $\pm 2 \text{ kcal mole}^{-1}$. Fielding and Pritchard²⁵ reported a value of $72 \pm 2 \text{ kcal mole}^{-1}$ for $\Delta H_f^\circ(\cdot\text{Ph}, \text{g})$ which is incorporated in this investigation in calculating the mean bond energy, $\bar{E}(\text{Sn}-\text{Ph})$.

Enthalpy of formation of Sn (g)

A value of $72.2 \pm 0.5 \text{ kcal mole}^{-1}$ ²⁶ is accepted for the enthalpy of formation of gaseous tin.

Average bond dissociation energy of (Sn-C) in tetraphenyltin

The mean value of the bond dissociation energy of the metal-to-carbon bond in organometallic compounds containing the metal M of valence n and the monovalent radical R, is given by:

$$\bar{E}(\text{M-C}) = \frac{1}{n} \overline{\Delta H_f^{\circ}(\text{R, g}) + \Delta H_f^{\circ}(\text{M, g}) - \Delta H_f^{\circ}(\text{MR}_n, \text{g})} \quad (\text{IV-3})$$

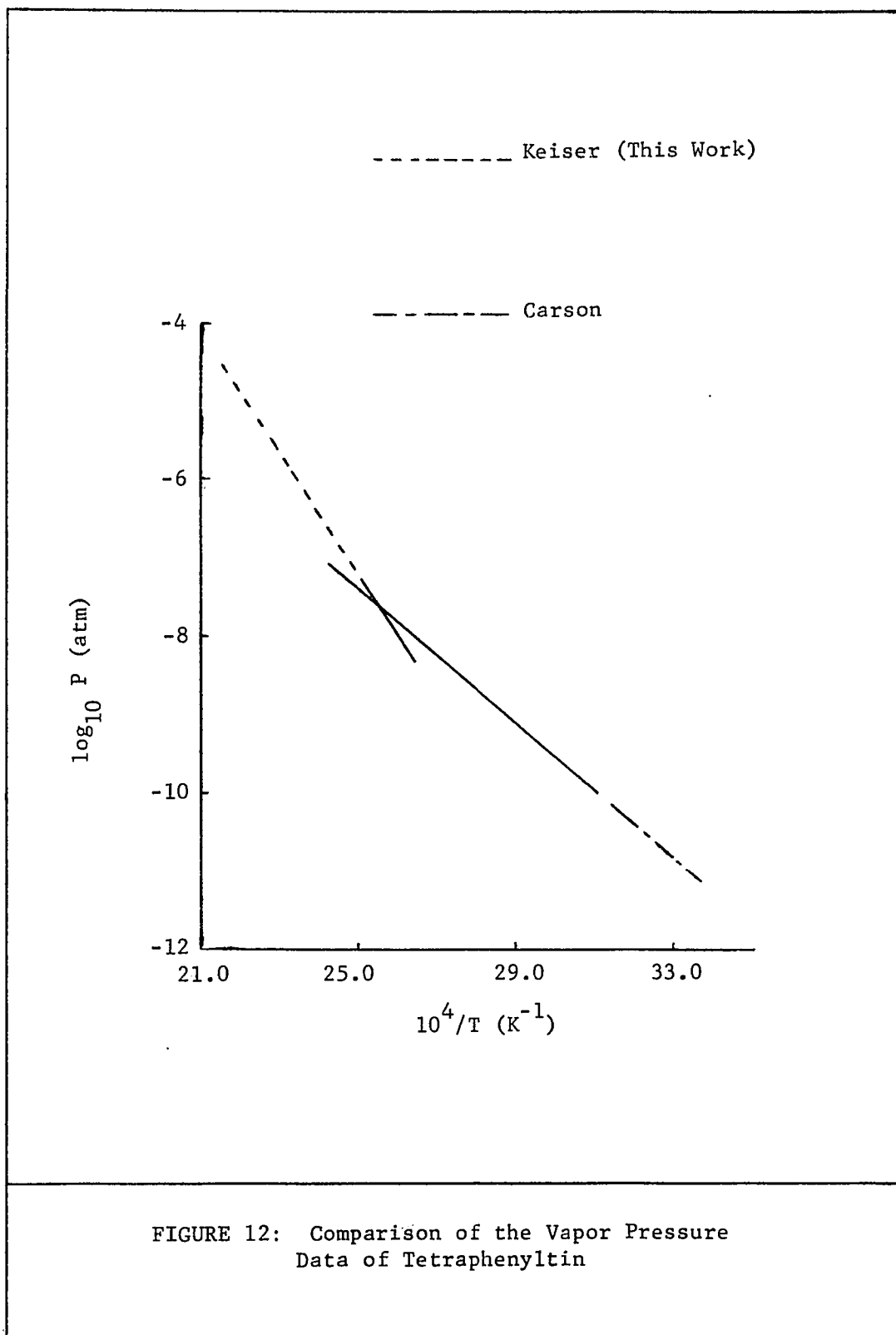
The mean bond dissociation energy of Sn-C in tetraphenyltin is calculated to be $\bar{E}(\text{Sn-C}) = 56.0 \pm 2.5 \text{ kcal mole}^{-1}$ according to:

$$\begin{aligned} \bar{E}(\text{Sn-C}) &= \frac{1}{4} \overline{\Delta H_f^{\circ}(\cdot\text{Ph, g}) + \Delta H_f^{\circ}(\text{Sn, g}) - \Delta H_f^{\circ}(\text{SnPh}_4, \text{g})} \\ &= \frac{1}{4} \overline{(4)(72 \pm 2) + (72.2 \pm 0.5 - 136.5 \pm 1)} \\ &= 56.0 \pm 2.5 \text{ kcal mole}^{-1} \end{aligned} \quad (\text{IV-4})$$

This value differs from the value of $61.4 \pm 2 \text{ kcal mole}^{-1}$ calculated by Pope and Skinner²² based upon the low value of the enthalpy of sublimation by Carson et. al.¹⁶

Discussion

The vapor pressure of tetraphenyltin at 298 K and the enthalpy of sublimation reported by Carson et al.¹⁶ were incorporated in a Clausius-Clapeyron equation to derive a value of 2.5 eu for the entropy of sublimation. A comparison of Clausius-Clapeyron plots based on Carson's data and the combined Knudsen-effusion data of experiments 2, 3 and 7 is presented in Figure 12. Such comparison shows a significant discrepancy between the two sets of data. This disagreement cannot be explained in terms of dissociative sublimation in the present study as indicated by the agreement between the simultaneous measurements of the vapor pressure by Knudsen-effusion and torsion-recoil methods. Extrapolation of the high temperature plot of this study to room temperature leads to a rather much lower pressure than that reported by Carson, et. al. A high vapor pressure and a low enthalpy of sublimation could be attributed to



incomplete degassing, the most common source of error in vapor pressure determination³¹, or to improper configuration of the experimental arrangement of effusate collection on a target.

The reliability of the data from the present investigation is supported by the following arguments:

The measured enthalpies of sublimation of triphenylgallium and triphenylindium are reported to be 32.9 ± 0.9 and 33.6 ± 0.4 kcal mole⁻¹, respectively.²⁷ These values are comparable with those of planar hydrocarbons, such as anthracene and pyrene, for which the enthalpies of sublimation correspond to a value of ca. 1.75 kcal mole⁻¹ per carbon atom.²⁸ The enthalpies of sublimation of non-planar compounds of related symmetry are rather lower than those of planar molecules. The measured enthalpies of sublimation of non-planar molecules such as triphenylarsenic (23.5 kcal mole⁻¹), triphenylantimony (25.4 kcal mole⁻¹)²⁹, triphenylboron (26.6 ± 0.3 kcal mole⁻¹)²⁷, and triphenylmethane (24.1 ± 1.0 kcal mole⁻¹)³⁰ are in accordance with this. On the basis of these limited examples one may surmise that for such non-planar systems, the enthalpies of sublimation correspond to a value of ca. 1.4 ± 0.1 kcal mole⁻¹ per carbon atom. Accordingly, tetraphenyltin should have an enthalpy of sublimation equal to 33.6 ± 2.4 kcal mole⁻¹. This value is of the same order as the measured enthalpy of this work.

The additivity of the enthalpy of sublimation in terms of uniquely defined group increments:

$$\Delta H_S^O = H_S^O (R\cdot) + H_S^O (X\cdot)$$

where $H_S^O (R\cdot)$ is the standard enthalpy of sublimation increment for

a given alkyl group $R\cdot$, and $H_S^O(X\cdot)$ that of some functional group $X\cdot$ had been suggested by Bondi.³¹ For alkyl aromatics he suggested a value of $10 \text{ kcal mole}^{-1}$ for $H_S(Ph\cdot)$ with a sharp decrease in the magnitude of the ring increment with increasing size of the molecule. He pointed out that his method errs consistently on the high side. A source of bias towards the high side is the fact that most increments were obtained on molecules of simple shape which are packed more tightly in their crystals than are complex molecules. The standard enthalpy of sublimation increments for functional groups containing tin in stannanes e.g. tetraalkyl is $1.5 \text{ kcal mole}^{-1}$ for tetravalent tin. The corresponding value for tin in tetraphenyltin is expected to be lower. This is based on the correspondence between the respective values for arsenic and antimony, where $H_S^O(As)$ equals $2.4 \text{ kcal mole}^{-1}$ in trialkylarsine and $H_S^O(As)$ approximately equals 0 in triarylarsine, and $H_S^O(Sb)$ equals $3.3 \text{ kcal mole}^{-1}$ in trialkylstibine and $H_S^O(Sb)$ equals $2.0 \text{ kcal mole}^{-1}$ in triarylstibine.

Aihara³² applied the additivity rule to the lattice energy of organic crystals and allotted a value of $9.0 \text{ kcal mole}^{-1}$ to the phenyl group contribution to the lattice energy. This value was determined by dividing the enthalpy of sublimation of biphenyl ($18.1 \text{ kcal mole}^{-1}$) by two which is very close to the heat of sublimation of benzene ($9.2 \text{ kcal mole}^{-1}$) attributed to Trieschmann.³⁷

Summary

Vapor-pressure measurements of tetraphenyltin, in the temperature range 403 to 462 K, lead to the Clausius-Clapeyron equation

$$\log_{10} P \text{ (atm)} = 12.739 \pm 0.428 - (7887 \pm 186) T^{-1} \quad (\text{IV-5})$$

The enthalpy and entropy of sublimation derived from this equation are

$$\Delta H_T^{\circ} = 36.1 \pm 0.1 \text{ kcal mole}^{-1}$$

and

$$\Delta S_T^{\circ} = 58.3 \pm 2.0 \text{ eu}$$

where $\bar{T} = 433\text{K}$.

The average bond energy, \bar{E} (Sn-C), in tetraphenyltin calculated from the available thermodynamic data and the present sublimation data is $56.0 \pm 2.5 \text{ kcal mole}^{-1}$.

The vapor pressure, P_{γ} , measured directly by the torsion-recoil method, is higher than the vapor pressure, P_K , determined indirectly from measurements of the rate of mass effusion. The discrepancy between P_{γ} and P_K , although based on one experiment, is not attributed to dissociative sublimation but, probably, due to a systematic difference between the two procedures.

On the basis of the sublimation data of tetraphenyltin and the limited data available on the sublimation of non-planar hydrocarbons it is surmised that the contribution to the enthalpy of sublimation of non-planar hydrocarbons is of the order of $1.4 \pm 0.05 \text{ kcal mole}^{-1}$ per carbon atom as compared with the corresponding value of $1.75 \text{ kcal mole}^{-1}$ in planar hydrocarbons.

CHAPTER V

VAPOR PRESSURES AND THERMODYNAMIC PROPERTIES OF HEXAPHENYLDITIN

Literature Review

The vapor pressure of hexaphenylditin and its temperature dependence have not been cited in the literature in any temperature range.

Material

Hexaphenylditin was a sample of the commercially available compound from Alpha Inorganics, Inc., used without recrystallization. Purity of the commercial sample was established by comparison of its melting point with that of a recrystallized sample from a solution of benzene. The melting point of the commercial and recrystallized samples were 229.5-232 C and 230-232 C, respectively, as compared with the literature value of 230-232 C.³³

Experimental Measurements

Vapor-pressure measurements were performed by use of the apparatus and according to the procedure described in Chapter III. A typical experiment was started similar to that of tetraphenyltin, except for heating to 230 C prior to measurements in the temperature range of 170 to 230 C.

Results

The saturated vapor pressure in equilibrium with solid hexaphenylditin was determined from measurements of the rate of effusion in one experiment and from simultaneous measurements of the rate of effusion and torsion recoil in two experiments. Aluminum cells, of different parameters, were used in all three experiments. The vapor pressures were calculated according to equations (II-7) and (II-12) assuming the monomeric vapor species of molecular weight 700.02 g mole⁻¹ for the mass effusion data. Least-squares analyses of the data, using an IBM 1620 Computer, gave the linear Clausius-Clapeyron equations which represent the vapor pressure of hexaphenylditin. The experimental data, the computed vapor pressures, and Clausius-Clapeyron equations are listed in Tables X-XIV and presented graphically in Figures 13-17. The second-law enthalpies and entropies of sublimation obtained from the above analyses are summarized in Table XV. Also listed in this table are the values of log P and standard deviations at the median temperature 475 K.

A composite least-squares analysis of all points of log P_K vs T⁻¹, in experiments 4 to 6, and of log P_γ vs T⁻¹, in experiments 5 and 6, were performed. The resulting Clausius-Clapeyron equations presented graphically in Figures 18 and 19 are

$$\log P_K = (14.082 \pm 0.124) - (9399 \pm 59)T^{-1} \quad (V-1)$$

$$\log P_\gamma = (14.087 \pm 0.276) - (9373 \pm 42)T^{-1} \quad (V-2)$$

They lead to the enthalpy and entropy of sublimation values of 43.00 ± 0.03 kcal mole⁻¹ and 64.4 ± 0.6 eu, respectively.

TABLE X

Knudsen-Effusion Data of Hexaphenylditin, Experiment No. 4^a

Pt. No.	Weight Loss w (g x 10 ³)	Time t (min)	Temperature T (K)	Pressure P (atm)	10 ⁴ /T (K ⁻¹)	-log P
1	1.79	10.0	483.8	4.535 x 10 ⁻⁶	20.670	5.343
2	1.48	395.0	443.8	9.091 x 10 ⁻⁸	22.532	7.041
3	1.23	250.0	448.1	1.196 x 10 ⁻⁷	22.316	6.922
4	1.74	200.0	452.8	2.138 x 10 ⁻⁷	22.086	6.670
5	2.04	150.0	458.3	3.354 x 10 ⁻⁷	21.822	6.475
6	4.40	180.0	463.6	6.068 x 10 ⁻⁷	21.573	6.217
7	2.21	55.0	467.8	1.003 x 10 ⁻⁶	21.375	5.999
8	5.85	80.0	475.4	1.838 x 10 ⁻⁶	21.035	5.736
9	7.10	25.0	489.6	7.242 x 10 ⁻⁶	20.424	5.140
10	20.10	50.0	493.3	1.029 x 10 ⁻⁵	20.270	4.988
11	12.46	85.0	482.9	3.713 x 10 ⁻⁶	20.761	5.430
12	20.40	30.0	500.1	1.753 x 10 ⁻⁵	19.996	4.756

$$\log_{10} P \text{ (atm)} = (13.690 \pm 0.217) - (9222 \pm 32) T^{-1}$$

a) Effective orifice area: $1.2330 \times 10^{-2} \text{ cm}^2$.

TABLE XI

Knudsen-Effusion Data of Hexaphenylditin, Experiment No. 5^a

Pt. No.	Weight Loss w ($g \times 10^3$)	Time t (min)	Temperature T (K)	Pressure P (atm)	$10^4/T$ (K^{-1})	$-\log P$
1	11.54	35.0	485.1	5.334×10^{-6}	20.616	5.273
2	2.46	170.0	453.3	2.268×10^{-7}	22.062	6.644
3	2.06	180.0	450.7	1.786×10^{-7}	22.189	6.748
4	1.51	100.0	454.6	2.363×10^{-7}	21.998	6.626
5	2.15	95.0	458.0	3.551×10^{-7}	21.836	6.450
6	3.36	85.0	463.4	6.245×10^{-7}	21.578	6.204
7	7.40	100.0	469.2	1.177×10^{-6}	21.314	5.929
8	8.44	70.0	474.4	1.928×10^{-6}	21.078	5.715
9	16.12	85.0	479.3	3.049×10^{-6}	20.366	5.516
10	18.87	80.0	482.9	3.807×10^{-6}	20.709	5.419
11	35.21	80.0	488.7	7.147×10^{-6}	20.463	5.146
12	44.79	62.5	494.5	1.171×10^{-5}	20.222	4.932

$$\log_{10} P \text{ (atm)} = (14.068 \pm 0.232) - (9392 \pm 109)T^{-1}$$

a) Effective orifice area: $1.9345 \times 10^{-2} \text{ cm}^2$.

TABLE XII

Torsion-Effusion Data of Hexaphenylditin, Experiment No. 5^a

Pt. No.	Deflection S (inch)	Temperature T (K)	Pressure P (atm)	$10^4/T$ (K ⁻¹)	-log P
1	7.26	485.1	5.588×10^{-6}	20.616	5.253
2	1.53	469.2	1.178×10^{-6}	21.314	5.929
3	2.90	474.4	2.232×10^{-6}	21.078	5.651
4	3.70	479.3	2.848×10^{-6}	20.866	5.546
5	5.14	482.6	3.956×10^{-6}	20.709	5.403
6	10.92	488.7	8.405×10^{-6}	20.463	5.076
7	16.22	494.5	1.248×10^{-5}	20.222	4.904

$$\log_{10} P \text{ (atm)} = (14.178 \pm 0.944) - (9431 \pm 454) T^{-1}$$

a) Effective orifice area x moment arm: $3.2340 \times 10^{-2} \text{ cm}^3$.

Torsion constant, α : $0.9096 \text{ dyn cm rad}^{-1}$

TABLE XIII

Knudsen-Effusion Data of Hexaphenylditin, Experiment No. 6^a

Pt. No.	Weight Loss w (g x 10 ³)	Time t (min)	Temperature T (K)	Pressure P (atm)	10 ⁴ /T (K ⁻¹)	-log P
1	8.54	70.0	483.2	4.577 x 10 ⁻⁶	20.694	5.339
2	1.10	130.0	457.0	3.094 x 10 ⁻⁷	21.881	6.509
3	2.18	125.0	463.4	6.389 x 10 ⁻⁷	21.582	6.194
4	1.51	50.0	468.8	1.112 x 10 ⁻⁶	21.329	5.954
5	4.10	85.0	472.5	1.789 x 10 ⁻⁶	21.164	5.747
6	7.88	95.0	479.1	3.098 x 10 ⁻⁶	20.873	5.509
7	8.92	85.0	481.6	3.928 x 10 ⁻⁶	20.762	5.406
8	12.11	70.0	487.4	6.515 x 10 ⁻⁶	20.519	5.186
9	19.60	70.0	492.7	1.060 x 10 ⁻⁵	20.298	4.975
10	19.53	45.0	497.9	1.652 x 10 ⁻⁵	20.083	4.782
11	44.19	65.0	503.1	2.601 x 10 ⁻⁵	19.875	4.585

$$\log_{10} P \text{ (atm)} = (14.296 \pm 0.222) - (9493 \pm 107) T^{-1}$$

a) Effective orifice area: $8.330 \times 10^{-3} \text{ cm}^2$.

TABLE XIV

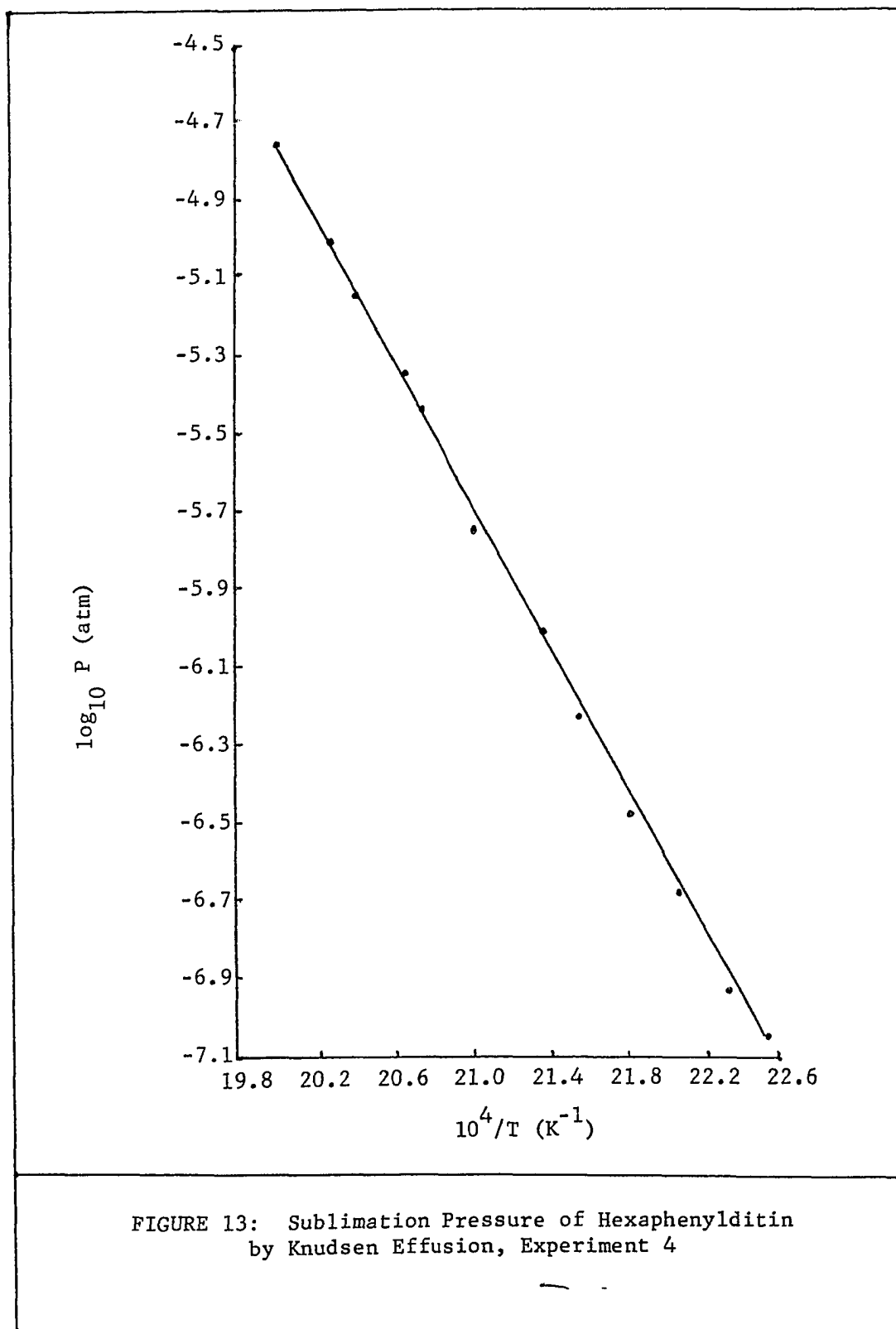
Torsion-Effusion Data of Hexaphenylditin, Experiment No. 6^a

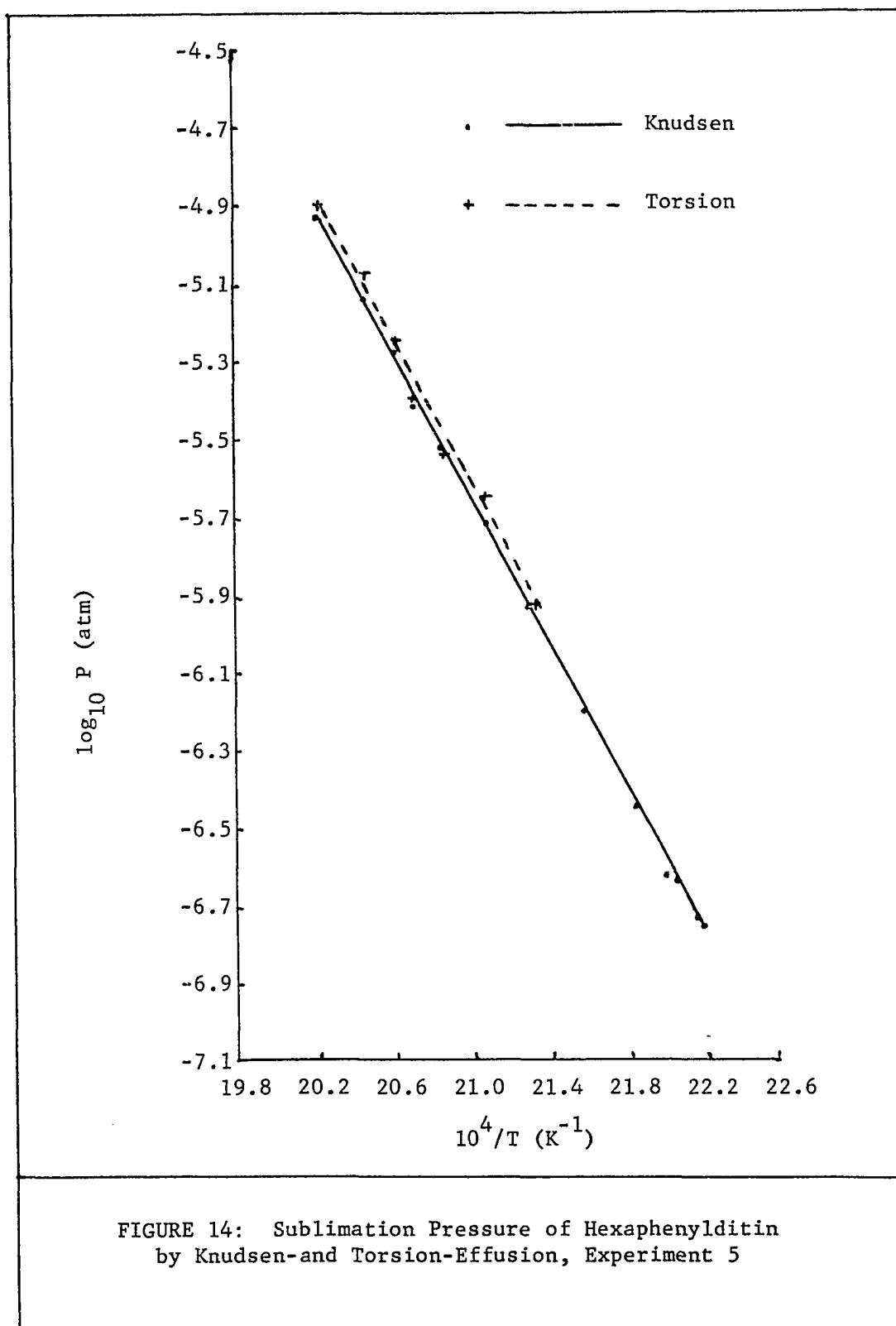
Pt. No.	Deflection S (inch)	Temperature T (K)	Pressure P (atm)	$10^4/T$ (K ⁻¹)	-log P
1	2.84	483.2	5.049×10^{-6}	20.694	5.297
2	0.43	463.4	7.645×10^{-7}	21.582	6.117
3	1.93	479.1	3.432×10^{-6}	20.873	5.465
4	2.31	481.6	4.107×10^{-6}	20.762	5.387
5	3.93	487.4	6.987×10^{-6}	20.519	5.156
6	6.55	492.7	1.165×10^{-5}	20.298	4.934
7	10.40	497.9	1.849×10^{-5}	20.083	4.734
8	17.05	503.1	3.031×10^{-5}	19.875	4.518

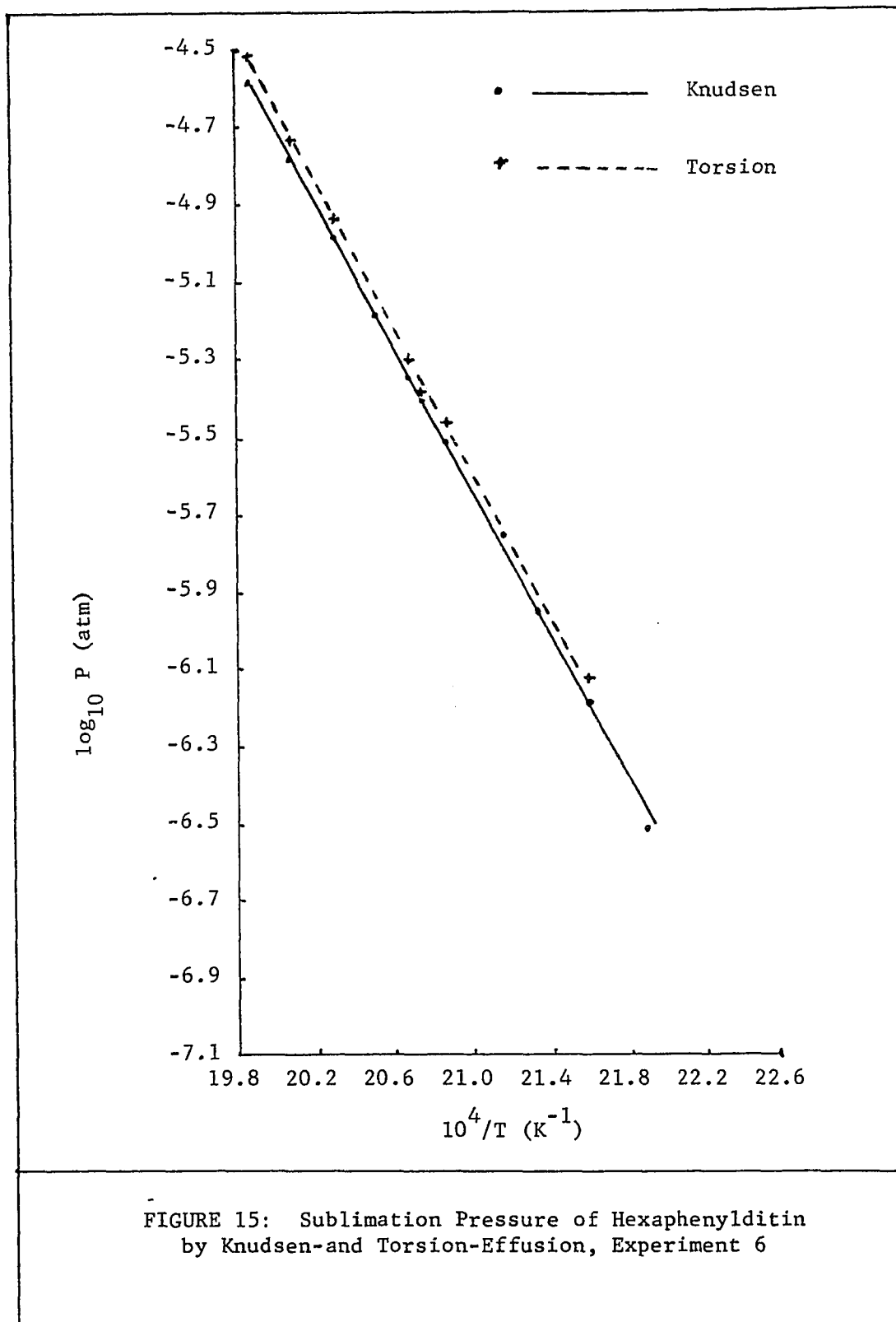
$$\log_{10} P \text{ (atm)} = (14.006 \pm 0.220) - (9330 \pm 107) T^{-1}$$

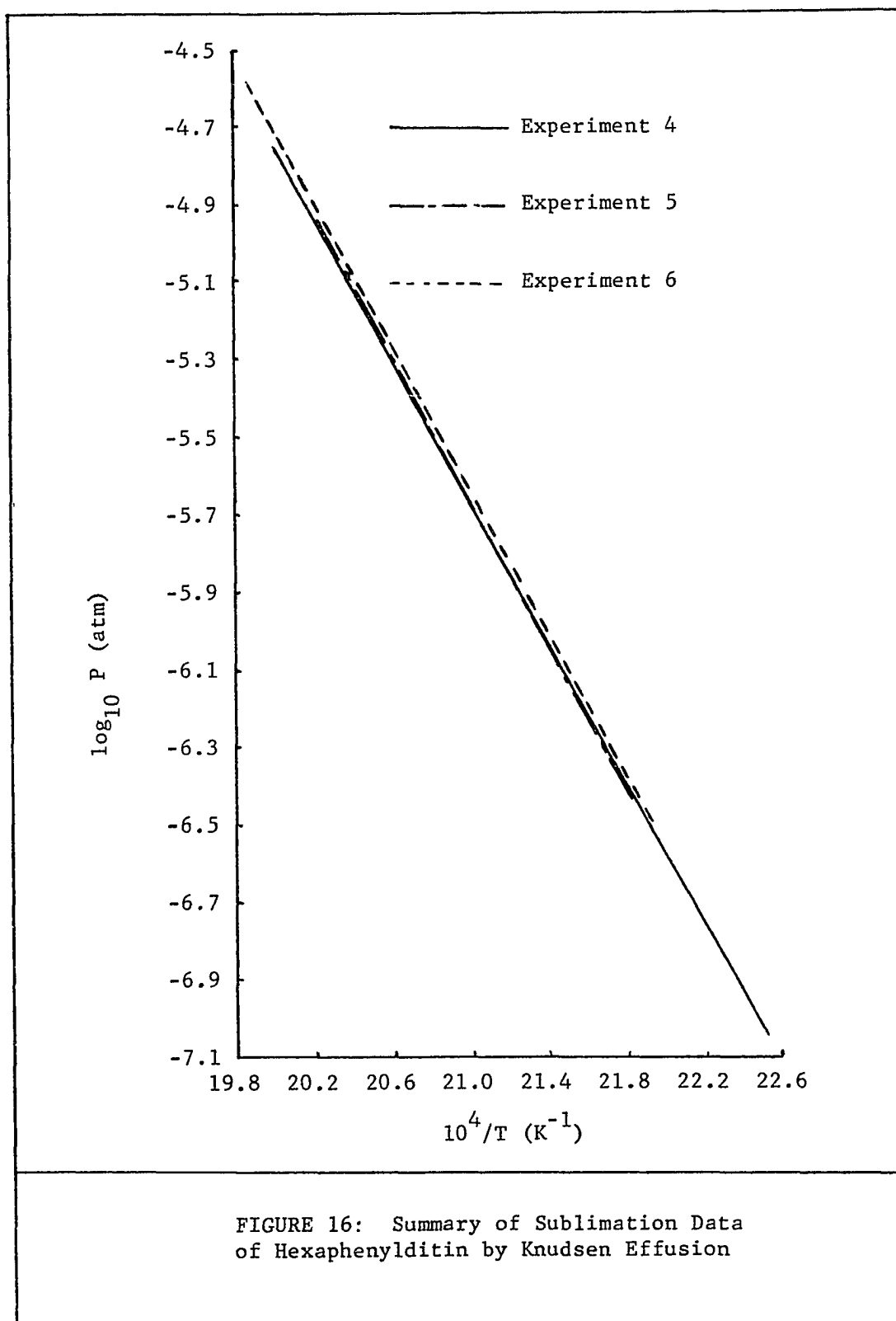
a) Effective orifice area x moment arm: $1.388 \times 10^{-2} \text{ cm}^3$.

Torsion constant, τ : $0.9002 \text{ dyn cm rad}^{-1}$









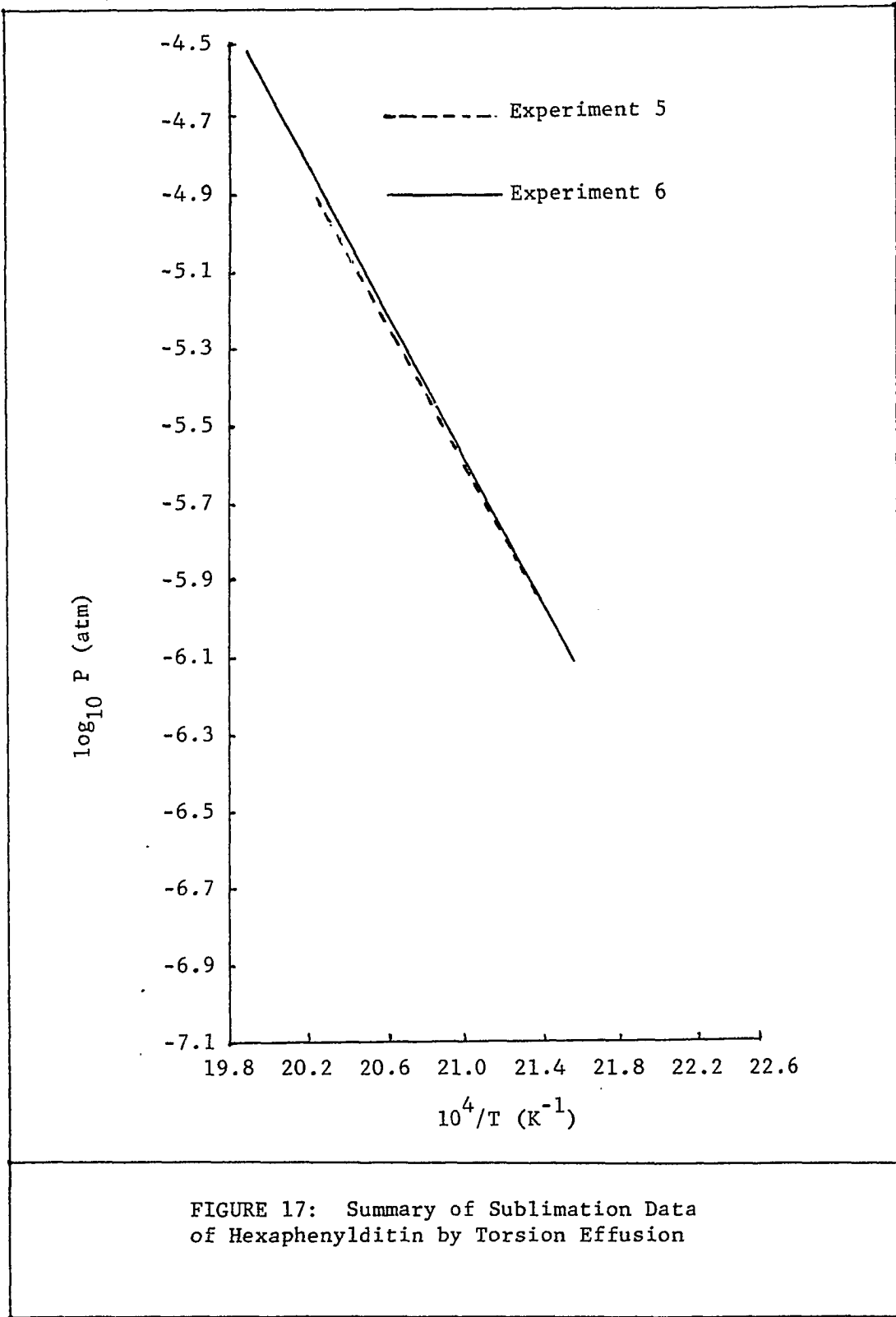
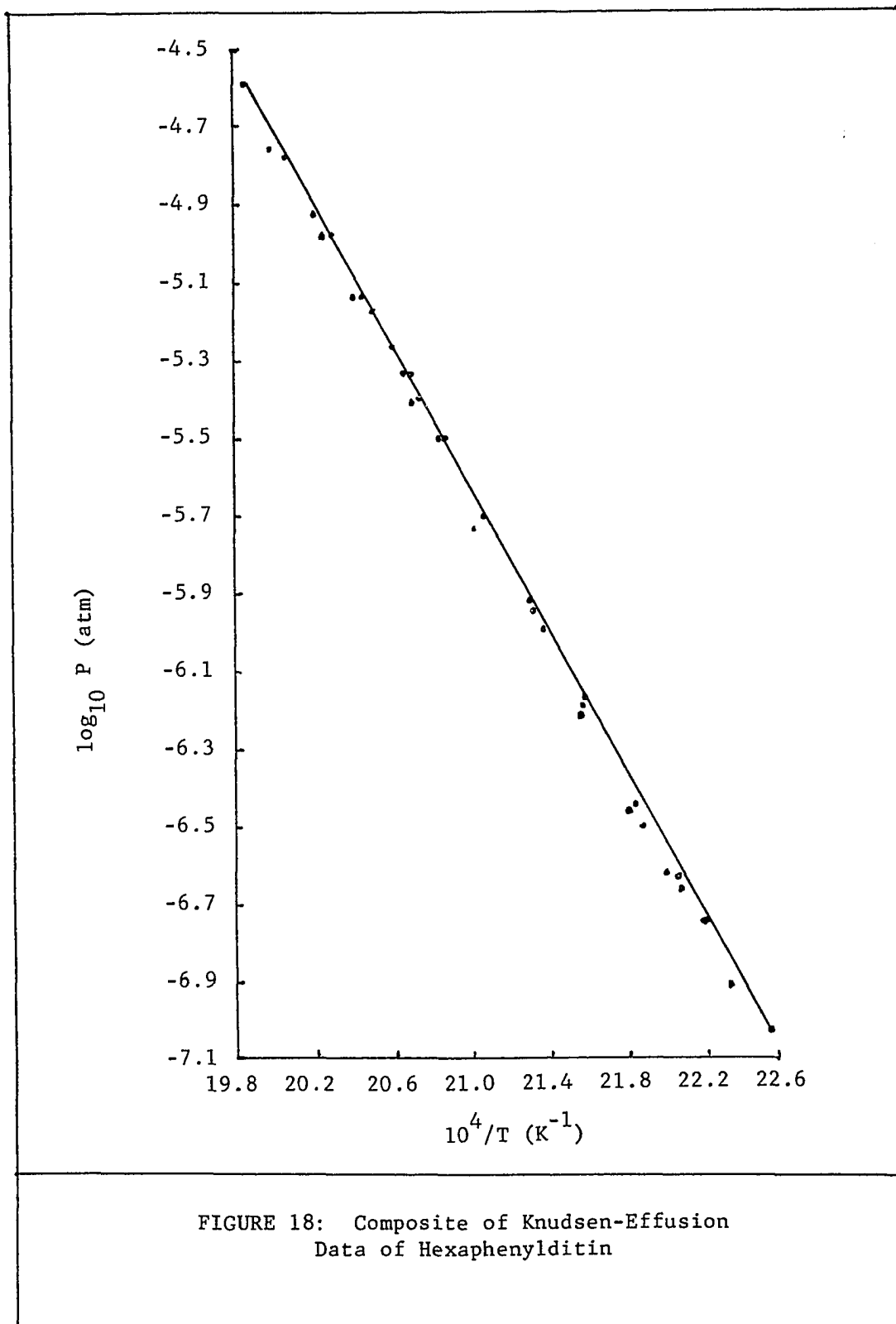


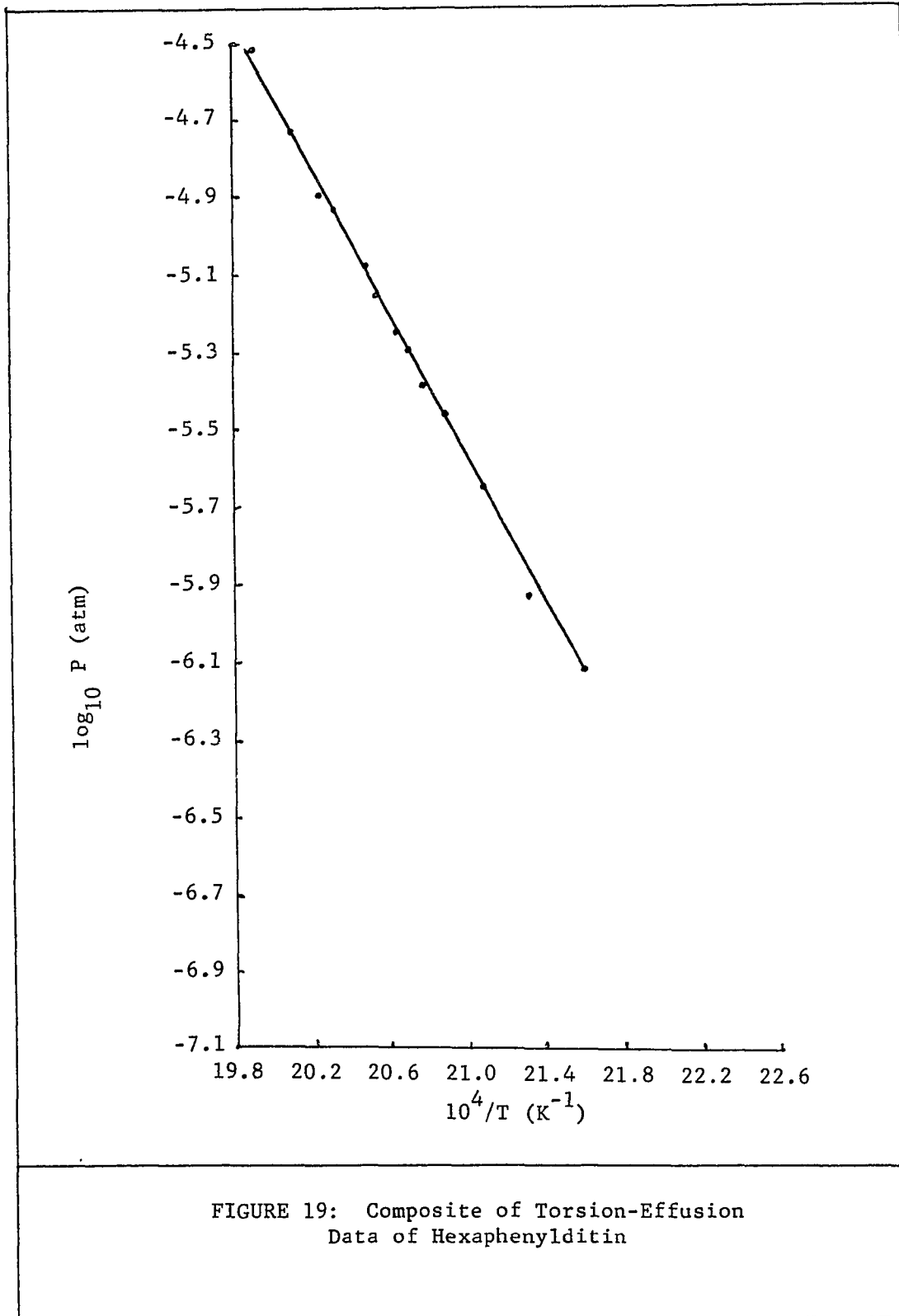
TABLE XV

Summary of Vapor-Pressure Data of Hexaphenylditin^a

Experiment No.	ΔH_T^0 (kcal mole ⁻¹)	ΔS_T^0 (eu)	$\log P_T$	P_T (atm)
4 Knudsen	42.2 ± 0.01	62.6 ± 1.0	-5.727	1.875 × 10 ⁻⁶
5 Knudsen	43.0 ± 0.05	64.4 ± 1.1	-5.704	1.978 × 10 ⁻⁶
6 Knudsen	43.4 ± 0.05	65.4 ± 1.0	-5.689	2.047 × 10 ⁻⁶
4,5,6 Knudsen	43.0 ± 0.03	64.4 ± 0.6	-5.705	1.972 × 10 ⁻⁶
5 Torsion	43.2 ± 0.20	64.9 ± 4.3	-5.676	2.107 × 10 ⁻⁶
6 Torsion	42.7 ± 0.05	64.1 ± 1.0	-5.636	2.310 × 10 ⁻⁶
5,6 Torsion	42.9 ± 0.20	64.5 ± 1.3	-5.646	2.262 × 10 ⁻⁶

a) $\bar{T} = 475$ K





Comparison of Simultaneous Measurements Via Torsion Recoil and Mass Effusion

The relationship between $P_{\mathcal{Z}}$ and P_K of hexaphenylditin is similar to that in the case of tetraphenylditin. Table XV and Figures 14 and 15 show that the average difference between $P_{\mathcal{Z}}$ and P_K corresponds to a value of 1.12 for $P_{\mathcal{Z}}/P_K$. The same arguments presented in connection with tetraphenylditin, concerning the acceptance of the monomer as the vapor species, and that the difference is related to configurational factors apply here as well.

Error Analysis

In Chapter IV an error analysis for the vapor-pressure data of tetraphenylditin was presented. The same error analysis is also true for hexaphenylditin. Therefore, the maximum propagated error in the Knudsen vapor pressure is $\pm 2.4\%$ and the maximum propagated error in the torsion vapor pressure is $\pm 4.9\%$. The corresponding errors in the calculated vapor pressures from the least-squares analyses are $\pm 4.9\%$, for P_K , and $\pm 4.2\%$, for $P_{\mathcal{Z}}$.

Derived Thermodynamic Properties

To calculate the thermodynamic properties of gaseous hexaphenylditin from the measurements associated with sublimation, the following data were employed.

Enthalpy of formation of solid hexaphenylditin

The heat of combustion of hexaphenylditin at 293 K was measured

by Lautsch et. al.³⁴ to be $4848.5 \pm 7.0 \text{ kcal mole}^{-1}$. For the enthalpy of formation they calculated the value, $\Delta H_f^\circ (\text{Sn}_2\text{Ph}_6, \text{s}, 298 \text{ K}) = 160.3 \text{ kcal mole}^{-1}$, based on the combustion data.

Enthalpy of formation of hexaphenylditin vapor

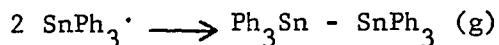
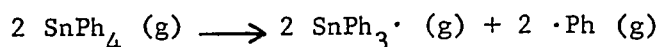
The enthalpy of gaseous hexaphenylditin is calculated from that of the solid and from the enthalpy of sublimation at 298 K, $\Delta H_s^\circ = 45.0 \pm 0.5 \text{ kcal mole}^{-1}$, to be $205.3 \pm 0.5 \text{ kcal mole}^{-1}$. This value accounts for a correction of $2.0 \pm 0.5 \text{ kcal mole}^{-1}$ representing the difference between the enthalpy of sublimation at the median temperature of 475 K and the reference temperature of 298 K.

Average bond dissociation energy of Sn-C bond

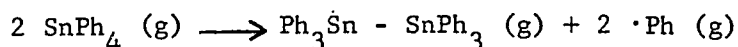
The average bond energy of Sn-C₆H₅ in hexaphenylditin is assumed to be the same as that in tetraphenylditin; the value of $\bar{E} (\text{Sn-C}) = 56.0 \pm 2.5 \text{ kcal mole}^{-1}$, derived in Chapter IV, is adopted.

The bond dissociation energy of Sn-Sn in hexaphenylditin

The bond dissociation energy of Sn-Sn is calculated from the thermodynamic properties of the following processes:



which are equivalent to:



Using $136.5 \pm 1 \text{ kcal mole}^{-1}$, for $\Delta H_f^\circ (\text{SnPh}_4, \text{g})$, $72 \pm 2 \text{ kcal mole}^{-1}$ for $\Delta H_f^\circ (\text{Ph}\cdot, \text{g})$, and $205.3 \pm 0.5 \text{ kcal mole}^{-1}$ for $\Delta H_f^\circ (\text{Sn}_2\text{Ph}_6, \text{g})$,

the enthalpy of the above reaction ΔH° is related to the bond dissociation energy of Sn-Sn according to:

$$\Delta H^\circ = -E (\text{Sn-Sn}) + 2 \bar{E} (\text{Sn-C}) \quad (\text{V-3})$$

But,

$$\Delta H^\circ = \Delta H_f^\circ (\text{Sn}_2\text{Ph}_6, \text{g}) + 2 \Delta H_f^\circ (\cdot\text{Ph}, \text{g}) - 2 \Delta H_f^\circ (\text{SnPh}_4, \text{g}) \quad (\text{V-4})$$

Thus,

$$E (\text{Sn-Sn}) = 2 \bar{E} (\text{Sn-C}) - \Delta H^\circ$$

or,

$$E (\text{Sn-Sn}) = 2 \bar{E} (\text{Sn-C}) + 2 \Delta H_f^\circ (\text{SnPh}_4, \text{g}) - \Delta H_f^\circ (\text{Sn}_2\text{Ph}_6, \text{g}) - 2 \Delta H_f^\circ (\cdot\text{Ph}, \text{g}) \quad (\text{V-5})$$

which, upon substitution of the corresponding numerical values, yields a value of $E (\text{Sn-Sn}) = 35.7 \pm 2.5 \text{ kcal mole}^{-1}$.

Discussion and Conclusions

The observed vapor pressures of hexaphenylditin, obtained from the simultaneous measurements of mass effusion and torsional recoil, are consistent with the assumption that hexaphenylditin monomer is the predominant vapor species. Additional results, obtained through linear least-squares analyses of the experimental data, are the enthalpy and entropy of sublimation. The derived enthalpy of sublimation, $\Delta H_s^\circ = 45.0 \pm 0.5 \text{ kcal mole}^{-1}$, is lower than the estimated value based on the surmise that the contribution to the enthalpy of sublimation, in non-planar hydrocarbons is approximately $1.4 \pm 0.1 \text{ kcal mole}^{-1}$ per carbon atom. The estimated value of $50 \pm 4 \text{ kcal mole}^{-1}$ is expected to err on the high side for complex molecules.³¹

The bond energy of Sn-Sn bond in hexaphenylditin is calculated,

from the available thermodynamic data and the sublimation data of this work, to be 35.7 ± 2.5 kcal mole⁻¹. This value is consistent with the bond energy of Sn-Sn in organometallic compounds. Cot-trell³⁵ cited for E (Sn-Sn), in hexamethylditin, a value of 39 kcal mole⁻¹ attributed to Pedley et. al.³⁶ The relatively large uncertainty is due to the uncertainty in the heat of combustion of hexa-phenylditin (4848.5 ± 7.0 kcal mole⁻¹), reported by Leutsch et. al.³⁴ and to the average bond energy, \bar{E} (Sn-Ph) = 56.0 ± 2.5 kcal mole⁻¹, derived from the sublimation data of tetraphenyltin reported in Chapter IV of this thesis.

CHAPTER VI

RECOMMENDATIONS FOR FUTURE WORK

The apparatus described in this thesis requires certain improvements so that more reliable and reproducible information will become attainable. Such improvements concern the thermocouple and the light source of the optical lever system. The thermocouple may be fixed more rigidly in a permanent position. The same recommendations apply to the light source which should be mounted firmly to the scale used in measuring the torsional deflection. Also, the combined light source and scale assembly should be firmly joined to the balance table.

A systematic study of the vapor pressures of the rest of the polyphenyl compounds of group IV A is recommended. Such a study should lead to further information about the bond strength and thermodynamic properties of this class of compounds. These properties may aid in elucidating their structural differences, especially in the absence of structural data by other means.

BIBLIOGRAPHY

1. L. Pauling and D. M. Yost, Proc. Nat. Acad. Sci., Washington, 18, 414 (1932).
2. C. T. Mortimer, Reaction Heats and Bond Strengths, Addison Wesley Publishing Co., Inc., (1962).
3. H. A. Skinner, Advances in Organometallic Chemistry Vol. 2, F. G. A. Stone and R. West (eds.), Academic Press, N. Y. (1964), pp. 49-114.
4. F. W. Sears, An Introduction to Thermodynamics, The Kinetic Theory of Gases and Statistical Mechanics, Addison-Wesley Publishing Co., Inc., (1963), pp. 200-220.
5. M. Knudsen, Ann. Physik., 28, 75 (1909); 28, 999 (1909); 29, 179 (1909).
6. P. Clausing, Ann. Physik, 12(5), 961 (1932).
7. P. Clausing, Physica, 9, 65 (1929).
8. W. C. DeMarcus and E. H. Hopper, J. Chem. Phys., 23, 1344 (1955).
9. H. Mayer, Z. Physik, 52, 235 (1929); 58, 373 (1929); 67, 240 (1931).
10. M. Volmer, Z. Physik, Chem Bodenstein Festband, 863 (1931).
11. A. W. Searcy and R. D. Freeman, J. Am. Chem. Soc., 76, 5229 (1954).
12. D. A. Schulz and A. W. Searcy, J. Chem. Phys., 36, 3099 (1962).
13. J. L. Margrave, Physico-Chemical Measurements at High Temperatures, O. M. Bockris, J. M. White (eds.), Butterworth Scientific Publications, London, (1959) p. 230.
14. D. L. Hildenbrand and W. F. Hall, Proceedings of the International Symposium on Condensation and Evaporation of Solids, Gordon and Breach Publishing Co., N. Y., (1964) pp. 399-415.
15. K. M. Myles, Trans. AIME, 230, 736 (1964).
16. A. S. Carson, R. Cooper and D. R. Stranks, Trans. Farad. Soc., 58, 2125 (1962).

17. G. E. Coates and K. Wade, Organometallic Compounds Vol. 1, third edition, Methuen and Co. Ltd. London, (1967) p. 419.
18. J. R. McCreary and R. J. Thorn, J. Chem. Phys., 48, 3290 (1968).
19. A. W. Searcy and R. D. Freeman, J. Chem. Phys., 23, 88 (1955).
20. G. M. Rosenblatt and C. E. Birchenall, J. Chem. Phys., 35, 788 (1961).
21. J. H. Kim and A. Cosgarea Jr., J. Chem. Phys., 44, 806 (1966).
22. R. C. Poller, J. Inorg. Nucl. Chem., 24, 593 (1962).
23. E. A. Pope and H. A. Skinner, Trans. Farad. Soc., 60, 1042 (1964).
24. R. J. Kandel, J. Chem. Phys., 22, 1496 (1954).
25. W. Fielding and H. O. Pritchard, J. Phys. Chem., 66, 821 (1962).
26. R. Hultgren, R. L. Orr, P. D. Anderson and K. K. Kelley, Selected Values of Thermodynamic Properties of Metals and Alloys, John Wiley and Sons, (1963) p. 262.
27. N. N. Greenwood, P. G. Perkins and M. E. Twentymen, J. Chem. Soc., 2109 (1967).
28. R. S. Bradley and T. G. Cleasby, J. Chem. Soc., 1690 (1953).
29. H. A. Skinner, op. cit., p. 84.
30. G. R. Cuthbertson and H. A. Bent, J. Am. Chem. Soc., 58, 2000 (1936).
31. A. Bondi, J. Chem. Eng. Data, 8, 371 (1963).
32. A. Aihara, Bull. Chem. Soc. of Japan, 32, 1242 (1959).
33. G. E. Coates and K. Wade, op. cit. p. 466.
34. W. S. Lautsch, A. Trober, W. Zimmer, L. Mehner, W. Linck, H. M. Lehmann, H. Brandenburger, H. Korner, H. J. Metzschker, K. Wagner and R. Kaden, Z. Chem., 3, 450 (1963).
35. T. L. Cottrell, The Strengths of Chemical Bonds, second edition, Butterworth Scientific Publications, London, (1958) p. 259.
36. J. B. Pedley, H. A. Skinner, and C. L. Chernick, Trans. Farad. Soc., 53, 1612 (1957).
37. H. G. Trieschmann, Dissertation, Kiel (1935).